TECHNICAL MEMORANDUM

377

Ozone in ERA-40: 1991-1996

Antje Dethof and Elias Hólm

Research Department

ECMWF

August 2002

European Centre for Medium-Range Weather Forecasts
Europäisches Zentrum für mittelfristige Wettervorhersage
Centre européen pour les prévisions météorologiques à moyen terme

For additional copies please contact

The Library
ECMWF
Shinfield Park
Reading
RG2 9AX
library@ecmwf.int

Series: ECMWF Technical Memoranda

A full list of ECMWF Publications can be found on our web site under:
http://www.ecmwf.int/publications/

Abstract

This paper takes a first look at the quality of the ozone analysis in the ERA-40 project between 1991 and 1996. In the ERA-40 analysis system TOMS and SBUV data from various platforms are assimilated between 1991 and 1996. The analyzed total column ozone field is generally good and has a realistic seasonal cycle. The large scale structures of the analyzed stratospheric ozone are also reasonable. However, there are problems with the vertical structure of the analyzed ozone fields, particularly in the troposphere and in polar regions. These problems come from the background errors for ozone which are used in ERA-40 until October 1996 and which have significant anti-correlations between the stratosphere and the troposphere.

1 Introduction

Ozone is a prognostic variable in the ECMWF model and is included in the analysis system in a univariate way. The univariate treatment is chosen to minimize the effect of ozone on the rest of the analysis system. The ozone analysis is included in the ECMWF 40-year re-analysis project plan (ERA-40) (Simmons and Gibson 2000) for years when ozone observations are available. In this report we look at the ERA-40 ozone analysis, carry out some basic validation of the analyzed ozone field for the years 1991 to 1996, and highlight problems with the ozone analysis. Section 2 looks a the ozone model and analysis, section 3 lists the ozone observations used in ERA-40, section 4 presents results from validation studies using independent MLS data and ozone sonde profiles, section 5 discusses the background errors for ozone used in ERA-40 and presents results from single observation experiments, and section 6 gives a summary and conclusions.

2 Ozone model and analysis

2.1 Model

Ozone is fully integrated into the ECMWF forecast model and analysis system as an additional three-dimensional model and analysis variable similar to humidity. The forecast model includes a prognostic equation for the ozone mass mixing ratio O_3 $[kg/kg]$

$$\frac{dO_3}{dt} = R_{O_3} \tag{1}$$

where R_{O_3} is a parameterization of sources and sinks of ozone. Without such a source/sink parameterization the ozone distribution would drift to unrealistic values in integrations longer than a few weeks. The source/sink parameterization must maintain a realistic ozone distribution over several years of integration, without reducing the dynamic variability of ozone. In addition, we would like the parameterization to be able to create an Antarctic ozone hole when the conditions are right.

The parameterization used in the ECMWF model is an updated version of Cariolle and Déqué (1986), which has been used in the ARPEGE climate model at Météo-France. This parameterization assumes that chemical changes in ozone can be described by a linear relaxation towards a photochemical equilibrium. It is mainly a stratospheric parameterization. The relaxation rates and the equilibrium values have been determined from a photochemical model, including a representation of the heterogeneous ozone hole chemistry. The updated version of the parameterization (with coefficients provided by Pascal Simon, Météo-France) is

$$\begin{aligned} R_{O_3} &= c_0 + c_1(O_3 - \bar{O_3}) + c_2(T - \bar{T}) \\ &\quad + c_3(O_3^{\uparrow} - \bar{O_3}^{\uparrow}) + c_4(Cl_{EQ})^2 O_3, \end{aligned} \tag{2}$$

where

$$O_3^{\uparrow}(p) = -\int_p^0 \frac{O_3(p')}{g} dp'. \tag{3}$$

Here c_i are the relaxation rates and $\bar{T}$, $\bar{O_3}$, and $\bar{O_3}^{\uparrow}$ are photochemical equilibrium values, all functions of latitude, pressure, and month. Cl_{EQ} is the equivalent chlorine content of the stratosphere for the actual year, and is the only parameter that varies from year to year (see Figure1) . For the ECMWF model it was necessary to replace the photochemical equilibrium values for ozone with an ozone climatology (Fortuin and Langematz 1995) derived from observations. The ozone parameterization is only active in daylight, and the heterogeneous part is only turned on below a threshold temperature of 195 K.

2.2 Analysis

In the ERA-40 system there is no separate ozone analysis, but ozone is analyzed simultaneously with all the other analysis variables in the 3D-VAR system, and ozone sensitive observations are treated just like any other observation. In the 3D-VAR system, ozone is analyzed univariately, which means that the analysis increments of ozone and other variables are assumed to be uncorrelated. Ideally, we should take into account the correlation which exists between ozone increments and the dynamical increments and perform a multivariate analysis of ozone. However, in a multivariate 3D-VAR analysis the ozone sensitive observations will directly change the dynamic analysis variables as well as the ozone field. Since most of the ERA-40 ozone observations are being assimilated for the first time in a dynamic model, it is not known if the quality of the data is good enough not to affect the atmospheric state adversely. To prevent ozone sensitive observations from directly changing any variable other than ozone, a univariate treatment is chosen.

For similar reasons, model ozone is not used directly in the radiation calculations of the forecast model, where the ozone climatology of Fortuin and Langematz (1995) is used instead. The only way ozone can affect the dynamics is through the use of the model ozone in the radiance observation operators. In the ERA-40 model/analysis configuration this is a weak feedback, which should mostly improve the usage of radiance observations.

The main difficulty with the assimilation of the TOMS and SBUV retrieved ozone data, which are given as vertically integrated layers spanning several model levels, is how to distribute the analysis increments in the vertical. This distribution is controlled by the background error covariance matrix of the ECMWF 3D-VAR assimilation system. The vertical covariances directly determine the weights with which the layer increment is spread in the vertical and hence the shape of the resulting analysis increment profile.

The ozone background error covariances used in the ERA-40 system were determined statistically from an ensemble of analysis experiments. The observations used in each analysis were perturbed randomly according to the observation error. Differences between the background fields valid at the same time, but from different experiments are taken to be representative of the background error and give fields from which the background error statistics can be calculated (Anderson and Fisher 2001).

3 Observations

A comprehensive review of the availability and quality of ozone data from 1957 onwards can be found in the SPARC (1998) report on the assessment of trends in the vertical distribution of ozone. Ground-based Dobson instruments have been measuring ozone (at some stations) since 1957, whereas reliable ozone sondes have been launched (at some stations) since 1970. The first extensive series of satellite ozone measurements comes from the BUV (Backscatter UltraViolet) instrument on NIMBUS-4 (1970-1977). However, the global observation of ozone only began seriously in 1978 with the launch of the NIMBUS-7 satellite which had on board both a TOMS (Total Ozone Mapping Spectrometer) instrument and a SBUV (Solar Backscatter UltraViolet) instrument. Since 1978 there has been a near continuous record of ozone measurements from different TOMS and SBUV instruments, with the exception of 1995 and the first half of 1996, when no TOMS instruments were

operating. Another extensive satellite observation record comes from SAGE I/II (Stratospheric Aerosol and Gas Experiment) instrument, which has been measuring ozone since 1979.

Most of the ozone measuring instruments have never been used on a global scale for their whole recording span. For their use in ERA-40 it is essential that the whole recording series of a particular instrument type is internally consistent, including corrections for known drifts, biases, and jumps in the observations, as well as flagging of observations of lower quality. Of the above mentioned instrument types, TOMS, SBUV and SAGE have all been reprocessed for their whole recording period from 1978/9 onwards in an attempt to obtain a trend quality observation record. The BUV observations, which stretch back to 1970 (with some gaps), had not been reprocessed in time for the ERA-40 production (McPeters, personal communication). The SAGE data, while being of high quality with high vertical resolution, have a rather limited horizontal coverage. Other satellite instruments like GOME (Global Ozone Monitoring Experiment) and the instruments on the Upper Atmosphere Research Satellite (UARS) have observed ozone for a more limited time period, and have not all been reprocessed to trend-quality.

Ground-based measurements and ozone sondes also have a very limited coverage, and the ozone sondes measure infrequently. In addition, the ground-based and ozone sonde data have still not been reprocessed on a global scale, so that while some of the data are of excellent quality, the quality of others is unknown.

A further source of ozone sensitive data comes from the TOVS instrument, in particular HIRS channel 9. In ERA-40 it was decided to avoid the use of the ozone sensitive HIRS channels if possible, because this introduces a direct feedback from ozone back to temperature and the dynamics in the data assimilation.

In the light of the above, it was decided to use SBUV and TOMS data in ERA-40. TOMS gives high density horizontal coverage of total ozone, with ca. 200000 observations per day of which only ca. 20000 are used in the assimilation after the data have been thinned to reduce the effect of correlated data errors. The thinning is done by taking only every third scan of the TOMS data and only every third field of view along the selected scans. SBUV has lower horizontal coverage than TOMS, with ca. 1200 profiles per day, all of which are used. The profile information in SBUV is mainly in the middle and upper stratosphere. Although the original SBUV retrievals have twelve layers, the profile information above 1 hPa and below 16 hPa is determined mainly by climatology, and we have therefore combined these dependent layers to avoid correlated data, resulting in the following six layers: 0.1–1 hPa, 1–2 hPa, 2–4 hPa, 4–8 hPa, 8–16 hPa, 16 hPa–surface. Both SBUV and TOMS measure in daylight only.

The assimilation of ozone into ERA-40 Stream-1 started 1 January 1991, although it is planned to rerun the years 1989-1990 with ozone observations. Table 1 lists all the TOMS and SBUV data which are available during the ERA-40 period. Table 2 lists the TOMS and SBUV data that are actively assimilated in ERA-40. In general, TOMS data are not used at solar elevations less than 6° where the quality of the retrieval is less good (McPeters et al. 1996), and where the data producers have flagged the data to be of worse quality. SBUV data are not used at solar elevations less than 30° in the northern hemisphere (NH) where the bias between the data and the model is large, and they are not used where the data producers have flagged the data to be of worse quality.

4 Validation of the ozone field in ERA-40

4.1 Total column ozone

Even without the assimilation of ozone data the ECMWF model produces a realistic and stable ozone field, which is in broad agreement with gridded daily TOMS data. The top colour plot of Figure 2 shows the total column ozone field in Dobson Units (DU) on 10 February 1992 from a model run, which is started on 1 December 1991 and in which no ozone observations are assimilated. The bottom plot shows the TOMS data

Instrument	*Satellite*	*Years*
TOMS	NIMBUS 7	1978-1993
(Total ozone)	Meteor 3-5	1991-1994
	ADEOS-1	1996-1997
	Earth Probe	1996-
SBUV	NIMBUS-7	1978-1990
(6 layers)	NOAA-9	1985-1998
	NOAA-11	1989-1995, 1999-
	NOAA-14	1995-
	NOAA-16	2000-

Table 1: Ozone observations available for ERA-40.

Instrument	*Satellite*	*Years*
TOMS	NIMBUS 7	1.1.1991-7.5.1993
TOMS	METEOR 3	April 93 - Dec 1994
TOMS	Earthprobe	Sept. 96 -
TOMS	ADEOS 1	Oct. 96 -
SBUV	NOAA 11	Jan 1991 - Dec 1994
SBUV	NOAA 9	Jan 1995 -

Table 2: Ozone observations which are actively assimilated in ERA-40 between 1991 and 1996.

for the same day. Note that while the ozone field from ERA-40 is at 12z, TOMS needs 24 hours to cover the whole globe and the map shown is a daily composite.

Because the large scale ozone field is strongly determined by the atmospheric dynamics, and the wind analysis in the ECMWF system is good, the model captures the main features seen in the TOMS data even with the relatively simple chemistry parameterization. The zonal mean relative differences between the fields are less than 10 % over large parts of the globe. Compared to the TOMS data, the model underestimates total column ozone in the tropics and overestimates it at high latitudes.

The middle colour plot of Figure 2 shows the analyzed total column ozone field in DU on the same day from the ERA-40 production, in which TOMS total column ozone data and SBUV ozone layers are assimilated. The figure clearly shows that the analysis is drawing to the data and that the agreement between the analysis and the observations is very good. The zonal mean relative differences between the analyzed field and the TOMS data are now less than 2% everywhere.

The timeseries of zonal mean total column ozone in DU from ERA-40 and TOMS for the years 1989 and 1990 is shown in Figure 3. During this period no ozone observations are assimilated in the ERA-40 analysis system. The figure shows that the ECMWF model produces a stable ozone field, with a realistic seasonal cycle and no obvious trend. Again, we can see the model bias (underestimation of total column ozone in the tropics and overestimation at high latitudes), which is particularly pronounced in the NH in northern spring, and in the SH in southern spring, where the model fails to reproduce the very low ozone values of the Antarctic ozone hole.

Figure 4 shows the timeseries of zonal mean total column ozone in DU from 1991 to the end of 1996 from ERA-40 and TOMS data. From 1991 onwards, TOMS and SBUV data from various platforms are assimilated in the ERA-40 system. The differences between the analyzed ozone field and the TOMS data are now smaller than in 1989 and 1990, and the analyzed field reproduces well the seasonal variations seen in the TOMS data, as well as the inter-annual variability. For instance, lower total column ozone values are observed over large

parts of the globe during the years following the eruption of Mt. Pinatubo (15 June 1991). This decrease in total column ozone is seen in the analyzed ozone field, for example the lower total column values at high northern latitudes and in the circum-antarctic ozone maximum in 1992. The Antarctic ozone hole is also well captured in the ozone analysis.

4.2 Stratospheric ozone

Zonal mean cross sections of the analyzed stratospheric ozone and of ozone from SBUV in ppmm (parts per million mass) are plotted in Figure 5 for 3 January, 1 April, 6 July and 1 October 1994. The figure shows that the large scale zonal mean structure of the analyzed ozone in the stratosphere is reasonable. We can see that the gradient between the low tropospheric ozone values and the higher stratospheric values is well captured in ERA-40, as is the location of the tropical ozone maximum. However, the maximum values of the SBUV data in the tropics are generally slightly higher than the analyzed values. On 1 October 1994 we see mixing ratios as low as 4 ppmm around 20 hPa near the South Pole in the analyzed field. This is the time of the Antarctic ozone hole. While the analyzed total column values for this day agree well with TOMS data, the vertical structure at high southern latitudes does not look realistic. This will be discussed further in Section4.3.2.

4.3 Validation against independent observations

To further evaluate the quality of the ozone field in ERA-40, the analyzed fields are compared with independent observations, which are not used in the analysis. The independent observations used here are MLS data and ozone sondes. We concentrate on the years 1994 and 1996. The year 1994 is chosen because it is a good year for the ozone analysis in ERA-40, in which TOMS data from Meteor-3 and SBUV data from NOAA-11 are assimilated, and no change of satellite occurrs. The year 1996 is chosen as a bad year in the ERA-40 ozone analysis. It includes satellite changes, periods when no total column ozone data are assimilated, and periods when the SBUV data are not blacklisted correctly. During 1996 SBUV data from NOAA-9 are assimilated throughout the year, TOMS data from Earthprobe from September 1996 onwards, and TOMS data from ADEOS from October 1996 onwards.

4.3.1 Comparison with MLS data: Upper and middle stratospheric validation

MLS (Microwave Limb Sounder) was launched on board the Upper Atmosphere Research Satellite in September 1991 (Barath et. al. 1993). It measures vertical profiles of several atmospheric trace gases including ozone. The useful pressure range for ozone data is 46 - 0.46 hPa. Outside this range the MLS data have large uncertainties. The MLS data used for our comparisons were obtained from the British Atmospheric Data Centre (http://www.badc.rl.ac.uk/).

Figure 6 shows vertical cross sections of the zonal mean ozone field in ppmm for the pressure range between 46 and 0.5 hPa from ERA-40 (left plots) and from the MLS data (right plots) on 3 January, 1 April, 6 July and 1 October 1994. See Figure 5 for comparison with the zonal mean SBUV data for the same days.

Figure 6 confirms that the large scale vertical structure of the stratospheric ozone field is well captured in ERA-40 and that the location of the tropical ozone maximum of the analyzed ozone field agrees well with the MLS data. However, there are some differences between the fields. First, the tropical ozone maximum is generally larger in the MLS data than in the analyzed ozone field and placed at slightly higher altitude. The maximum values of the MLS data are slightly larger than those of the SBUV data, and are placed around 10 hPa compared to 7-9 hPa in the SBUV data. Secondly, in January 1994 the analyzed zonal mean values north of about 50°N are higher than the MLS ozone values between about 20 and 3 hPa. This difference is also seen in comparisons with ozone sondes (see Figure 14). At this time of year, no SBUV data are assimilated north of about 60°N.

Only TOMS data are assimilated here, and the differences could point to a problem in the distribution of the ozone analysis increment in the vertical or to a problem in the chemistry parameterization. Thirdly, in the upper stratosphere near the model top, the analyzed ozone is generally lower than the MLS ozone.

In 1996 (Figure 7) the main features seen when comparing MLS and analyzed ozone data are the same as in 1994. However, on 4 January 1996 the analyzed ozone field has relatively low values at high northern latitudes between 46 and 10 hPa which are not seen in 1994.

Next, we look at the annual cycle of the stratospheric and tropospheric ozone field, by comparing timeseries of the area averaged ozone fields plotted against pressure from ERA-40 and MLS data for the years 1994 and 1996. Area means are calculated for the latitude bands 60-90°N, 30°N-30°S, 60-90°S. In these timeseries the ozone field is plotted in mPa, which is proportional to the number density and allows one to compare the contributions from different layers to the total column in log pressure coordinates. The stratospheric ozone maximum appears at a lower altitude when expressed in mPa than when expressed as a mixing ratio, reflecting where the number density is larger.

In 1994, for 90-60°N (Figure 8) the ozone maximum is located between 50-70hPa. The largest values of the ozone maximum are found in March and April and the lowest values between July and September. This seasonal cycle is similar to that of the MLS data. However, the analyzed ozone maximum is found at slightly higher altitudes than the ozone maximum in the MLS data, leading to large relative differences between the data sets between 50-100 hPa. The timeseries of the relative differences confirms what we already saw in the individual cross sections. Near the model top the analyzed ozone is generally lower than the MLS ozone. Between about 0.5 - 40 hPa the analyzed ozone is higher than the MLS ozone, with the exception of the pressure range between 2 - 20 hPa between May and October. The largest differences between the analyzed ozone field and the MLS data are found in the troposphere. Even if the quality of the MLS data is not very good at these levels where they mainly reflect climatology, the comparison suggests that the analyzed ozone is much too low around 200 hPa, especially between September and December.

Between 30°N-30°S (Figure 9) the ozone maximum is located around 20 hPa and there is less seasonal variation than at higher latitudes. The MLS data have slightly larger values at the ozone maximum than the analyzed field and they show a layer of low ozone values between 40-50 hPa, which is not seen in ERA-40. However, this layer is at the bottom end of the 'good' MLS range, so one should be careful when interpreting it. It is not seen in ozone sonde profiles from the Hawaiian station Hilo (Figures 16 and 21) and might point to a problem in the MLS data. As at the higher latitudes, the largest differences between ERA-40 and MLS ozone are found below 50 hPa. We see low analyzed ozone values in the upper troposphere and higher analyzed values between 300-400 hPa, which is confirmed by the comparisons with the Hilo ozone sondes.

For 60-90°S (Figure 10) the ozone maximum is located between about 70-40 hPa and the largest values occur between March and July and from November to January. Between September and November the analyzed field has very low values up to 50 hPa marking the Antarctic ozone hole, while having slightly larger values near the surface. Unfortunately, there are not many MLS observations available during this period for comparison. Between January and April the analyzed ozone values are too low in the troposphere.

In 1996 many features are similar to 1994 (Figures 11 to 13). However, at 60-90°N (Figure 11) between January and May we see larger differences between the analyzed field and the MLS data than in 1994. The analyzed field has higher values at the ozone maximum around 50-70 hPa, very low ozone values in the upper troposphere, and higher values at the bottom of the pressure range. This layer of low ozone in the upper troposphere is also seen between 60-90°S.

While the timeseries show that the analyzed stratospheric ozone field has a realistic seasonal cycle and also captures well latitudinal differences in the altitude of the ozone maximum, there are large differences between the ERA-40 and MLS data below 50 hPa, particularly in the upper troposphere. Because the quality of the MLS data in this altitude range is not very good, we use additional data in form of ozone sondes for the validation of

Station	*Latitude*	*Longitude*
Ny-Aalesund	78.93	11.95
Hohenpeissenberg	47.80	11.0
Hilo	19.71	-155.08
Lauder	-45.05	169.68
South Pole	-89.99	-24.8

Table 3: Geographical locations of ozone sonde stations.

the analyzed ozone field below 50 hPa.

4.3.2 Comparison with ozone sondes: Tropospheric and lower stratospheric validation

Ozone profiles from ERA-40 are compared with ozone sonde profiles from the following five stations: Ny-Aalesund, Hohenpeissenberg, Hilo, Lauder and South Pole. The geographical locations of these stations are listed in Table 3. The ozone sondes are obtained from the Network for the Detection of Stratospheric Change (http://www.ndsc.ncep.noaa.gov/). Monthly mean ozone profiles and standard deviations are calculated for these stations for January, April, July and October 1994 and 1996. A simple quality check is carried out for the sondes, and sondes that do not reach 40 hPa are discarded. The ERA-40 ozone profiles are the analysis profiles from the grid point closest to the sonde location and from the closest analysis time.

The ozone profiles for 1994 are shown in Figures 14 to 18. The profiles from the NH stations Ny-Aalesund (Figure 14) and Hohenpeissenberg (Figure 15) show that the shape and the location of the ozone maximum is relatively well captured by the analyzed ozone profiles. However, the model ozone is generally too high in the lower troposphere, and here the differences are largest in January and April. This confirms the differences seen between the analyzed ozone field and the MLS data (Figure 8). In October the analyzed profiles show very low ozone values near 200 hPa, while the ozone sonde values are much higher. Again the sondes agree better with the MLS data than the analyzed profiles.

The tropical profiles from Hilo (Figure 16) also show an overestimation of tropospheric ozone in January, but in July and October they agree better in the troposphere than the profiles from the two NH stations. At Hilo, both the altitude and the magnitude of the ozone maximum are underestimated by the analyzed profiles. It is questionable how good the quality of the ozone sondes is above 20 hPa, but this underestimation in the analyzed profiles is in agreement with the model bias seen in the tropics, where the model total column ozone is generally too low.

The profiles for the SH station of Lauder (Figure 17) agree reasonably well in the stratosphere, with the exception of October when the ozone maximum of the analyzed profiles is too low compared to the sondes, while the analyzed ozone values below the ozone maximum are too high. In the lower troposphere the analyzed ozone values are again too large.

The profiles for the South Pole (Figure 18) show very large seasonal differences between October and the other three months. In January, April and July we see the ozone maximum at around 50 hPa, with values of about 14 mPa. The analyzed profile for July does not agree well with the sondes. The altitude of the analyzed ozone maximum is too low, there is a kink in the profile around 20 hPa, and the tropospheric values are too large. The October profiles show the Antarctic ozone hole. This seasonal change is well captured by the analyzed profiles, even though there are differences in the vertical distribution of analyzed and observed ozone. The stratospheric maximum is at a lower altitude in the model, and almost all the model ozone is removed between 60-200 hPa, whereas the sonde profiles have higher values between 100-300 hPa. The very low analyzed values around 200 hPa are unrealistic and seem to reflect the same problem that is seen at the other stations at various times of

year. The model values are too high in the troposphere below 300 hPa. Since the model has a large bias at this time of year, large corrections are needed in the analysis. Considering that the background error covariances for ozone do not account for the ozone hole, the analyzed profiles do not seem to be too bad.

The ozone profiles for 1996 are shown in Figures 19 to 23. The agreement between the analyzed profiles and the sonde profiles for the two NH stations (Figure 19 and Figure 20) is worse than in 1994, particularly in January and April 1996. The reason for this is likely to be the following. In 1996 SBUV data are not correctly blacklisted at high northern latitudes, but actively assimilated right up to the northern edge of the data coverage area (and also up to the southern edge of the data coverage area) in the first half of the year. Due to the large model bias in the NH at this time of year the analysis increments are large and lead to an overestimation of the ozone maximum, an almost complete depletion of the ozone in the upper troposphere and an overestimation of ozone in the lower troposphere. The blacklist mistake is corrected at the beginning of July 1996, so that the problem is not as severe in July and October. This can also be seen in the time series cross section of the analyzed ozone and MLS data in Figure 11.

The profiles from Hilo in 1996 (Figure 21) are very similar to the ones in 1994 and show again an overestimation of tropospheric ozone, and an underestimation of the altitude and the magnitude of the stratospheric ozone maximum in the analyzed profiles. The three sonde profiles for April show large variability.

The profiles for Lauder (Figure 22) show similar problems to the NH profiles in January and April 1996. As in the NH, the SBUV data are not blacklisted at low solar elevations and hence used in the analysis. This also causes problems for the analyzed profiles from the South Pole (Figure 23) where the analyzed ozone in January and April 1996 is almost completely depleted around 200 hPa, whereas the values in the lower troposphere are too large. In July 1996 the analyzed values are still too low around 200 hPa, but the difference is not as extreme as in January and April. As in 1994, the analyzed profiles for October capture the difference between the normal situation and the ozone hole situation. However, the ozone depletion in the analysis occurs at the wrong altitude, and seems to reflect problems with the ozone analysis rather than some true chemical depletion.

While many features seen from the sonde comparison show that the analyzed profiles are realistic over large parts of the stratosphere, the comparisons have highlighted several problems with the ozone analysis. Experiments in which no ozone observations are assimilated (e.g. ERA-40 ozone between 1989 and 1990) do not show the very low ozone values in the upper troposphere and the high values near the surface that we see in the ERA-40 profiles. From the ERA-40 profiles, we get the general impression that the larger the bias between the model and the data (and hence the larger the analysis increments), the worse the agreement between model and sondes. This suggests that while the analyzed total column values are reasonable, there are problems with the distribution of the analysis increments in the vertical, particularly in the troposphere and at high latitudes.

5 Background errors for ozone

The main difficulty with the assimilation of total column ozone data, such as the TOMS data, or data in relatively broad layers, such as the SBUV data, is how to spread the analysis increments in the vertical. In 3D-VAR, this is done by distributing the increments in the vertical with a weight proportional to the vertical background error covariances. The comparisons of the analyzed ozone profiles and the ozone sondes suggest that there are problems with the background errors for ozone in ERA-40. To investigate this in more detail single observation experiments are carried out.

5.1 Single observation experiments

5.1.1 Vertical correlations for ozone in ERA-40

For a single observation the shape of the analysis increment is given by BH^t,

$$x_a - x_b = (\frac{y - Hx_b}{\sigma_o^2 + \sigma_b^2})BH^t, \tag{4}$$

where x_a is the analysis value, x_b the background value, y the observation, σ_o^2 the observation variance, σ_b^2 the observation equivalent of the background covariance, B the background error covariance matrix and H the observation operator. To investigate how the increment from one total column ozone observation is spread in the vertical, a single TOMS observation of 247 DU is placed at 57.56 latitude, -28.38 longitude on 25 January 1992, at 11.19 UTC. This observation is 66.7 DU lower than the background value. This experiment is referred to as Exp-A.

Figure 24 shows a vertical cross section through the analysis increment (in ppmm) at 28.4°E created by this TOMS observation. The total column first-guess value is 313.7 DU at the location of the observation, the final analysis is 303.3 DU, and hence the total column analysis increment is -13.4 DU. The absolute impact of the single TOMS observation is largest around model level 22 (about 45 hPa), where it acts to reduce the background value. However, the analysis increment is spread out over the whole depth of the model atmosphere. The wavenumber averaged vertical correlation matrix for ozone (Figure 25) shows that there are anti-correlations between some stratospheric levels and levels in the troposphere. These anticorrelations can cause an unrealistic distribution of the ozone increments in the vertical in some regions, leading to a depletion of ozone at around 200 hPa and a piling up of ozone at the surface.

5.1.2 Modified vertical correlations for ozone

In an attempt to improve the vertical distribution of the ozone increments, new background errors are calculated. The main differences between the new and the old background errors are an explicit removal of correlations between the stratosphere and the troposphere and some change in the effective variances of the errors at different levels (see Figure 26).

The single observation experiment is repeated with the modified covariances. This experiment is called Exp-B and the vertical cross section of analysis increment (in ppmm) created by the single TOMS observation is shown in Figure 27. The analysis increment is now more confined in the vertical than in Exp-A and there are no anti-correlations between the stratosphere and the troposphere, or between levels at and above the stratospheric ozone maximum. The maximum impact is still seen around 40 hPa. In Exp-B the total column first-guess value is 313.7 DU at the location of the observation, and the analysis value is 310.5 DU. Because the variances have also been modified the magnitude of the analysis increment is different in the two experiments. The vertical distribution of the analysis increments with the new covariances looks better than with the old ones, and the new covariances have been used in ERA-40 from 24 October 1996 onwards.

5.2 Ozone profiles from ERA-40 using the new background errors for ozone

To study the impact of the modified background errors analyzed ozone profiles are compared with profiles from ozone sondes from Ny-Aalesund for February 1997 (see Figure 28). The implementation of the new covariances improves the tropospheric part of the analyzed ozone profiles. The very low values in the upper troposphere are not seen any more and the overestimation near the surface is reduced. However, because the ozone increments

are now more confined in the vertical, the values at and above the stratospheric ozone maximum get reduced too much.

The fact that problems with the vertical distribution of ozone remain, highlights the need to replace the static observation errors for ozone by flow dependent ones, which take into account the local values of ozone when assigning the background errors. The static background errors are global averages, which mostly reflect the tropics. Regions where the background ozone values are much different from the tropics (see Figure28) are still found to have problems with the vertical distribution of ozone increments even after the stratosphere-troposphere anti-correlations have been removed. This problem is made even more severe by the fact that the ERA-40 ozone observations are column values: total columns for TOMS and for SBUV the lowest column is from 16 hPa to the surface. Over this vertical range, the ozone values decrease by up to four orders of magnitude from the ozone maximum to the minimum values in the troposphere. It is easy to see that a negative ozone column increment can create negative ozone in the troposphere, particularly when the tropospheric values are much lower than the typical tropical values. Negative values are actually reset to a low value by the analysis, but this leads to other systematic errors in the Polar analysis of ozone.

6 Conclusions

Ozone retrievals from various TOMS and SBUV instruments are assimilated in ERA-40 between 1991 and 1996. The resulting total column ozone field is generally good and agrees well with observations. Comparisons with independent MLS data show that the analyzed stratospheric ozone is also good over large parts of the stratosphere.

While the analyzed total column ozone field is of good quality, there are problems with the vertical structure of the analyzed ozone field, particularly in the troposphere. The shape of the analyzed ozone profiles strongly depends on the vertical background error covariances. The vertical correlation matrix for ozone used before October 1996 has anti-correlations between the stratosphere and the troposphere. In situations where the total column analysis increments are large these anti-correlations lead to an overestimation of ozone near the surface, a strong reduction of ozone in the upper troposphere and an overestimation of the stratospheric ozone maximum. This problem is particularly pronounced in the NH between January and April. On the basis of single observation experiments, new covariances have been designed and implemented on 25 October 1996. These covariances do not have the anti-correlations between the stratosphere and troposphere and the resulting analysis increment is more confined in the vertical. However, with the new background errors for ozone there are still problems in situations where the analysis increment is large, for example at high northern latitudes in winter, when the model has a positive bias compared to TOMS data. In these situations the ozone maximum in the analyzed profiles is much reduced compared to observations. Users of the ERA-40 data should be aware that there are problems with the vertical structure of the analyzed ozone field.

The validation studies have shown the need to replace the globally averaged, static observation errors by flow dependent ones, which take the local values of ozone into account when assigning background errors. Such flow-dependent covariances are currently being developed and will replace the current covariances in later stages of the ERA-40 production and possible reruns. ECMWF is considering a longer rerun covering the latter part of the ERA-40 period. Such a rerun would use the same basic analysis method and model resolution as the initial ERA-40 production, but with an updated version of the forecasting system and a revised ozone analysis.

As well as highlighting problems with the vertical distribution of ozone the validation studies also show that the underlying problem for the ozone analysis is the bias between the model and the data, which is large at certain times of year. This violates the crucial assumption made in data assimilation that observations and first guess fields are unbiased, and it illustrates the need for a bias correction of ozone data. Additional work is required to understand the reason for the model bias and how to reduce it.

The experiences gained in ERA-40 with the assimilation of ozone retrievals have been benifitial for the operational implementation of the ozone assimilation. Since February 2002, SBUV profiles from NOAA-16 and total column ozone retrievals from GOME on ERS-2 (provided by KNMI) have been assimilated in the operational system.

A final word of advice. When comparing the analyzed ozone field from different years it should be kept in mind that data from different satellites are assimilated between 1991 and 1996, and that there are periods when no data are assimilated or periods when no TOMS data are available. See Table 2 for details.

7 Acknowledgements

We owe many thanks to Adrian Simmons, Jean-Noël Thépaut and Sakari Uppala for discussions and suggestions.

References

Anderson, E. and M. Fisher (2001). Developments in 4D-Var and Kalman Filtering. *ECMWF Technical Memorandum 347*.

Barath, F.T. et al. (1993). The Upper Atmosphere Research Satellite Microwave Limb Sounder Instrument. *J. Geophys. Res.*, 98, 10751–10762.

Cariolle, D. and M. Déqué (1986). Southern hemisphere medium-scale waves and total ozone disturbances is a spectral general circulation model. *J. Geophys. Res.*, 91. 10825–10846.

Fortuin, J.P.F. and U. Langematz (1995). An update on the global ozone climatology and on concurrent ozone and temperature trends. *SPIE Proceedings Series*, Vol. 2311, "Atmospheric Sensing and Modeling", pp 207-216.

McPeters, R.D., Bhartia, P.K., Krueger, A.J., Herman, J.R., Schlesinger, B.M., Wellemeyer, C.G., Seftor, C.J., Jaross, G., Taylor, S.L., Swissler, T., Torres, O., Labow, G., Byerly, W. and R.P.Cebula (1996). Nimbus-7 Total Ozone Mapping Spectrometer (TOMS) Data products user's guide. *Nasa reference publication.* Available from ftp://daac.gsfc.nasa.gov/data/toms/documentation/tomsn7_ userguide.pdf.

Simmons, A.J. and J.K. Gibson (2000). The ERA-40 project plan. *Era-40 Project Reoprt Series 1*.

SPARC Report No. 1 (1998). SPARC/IOC/GAW Assessment of Trends in the Vertical Distribution of Ozone. Editors N. Harris, Hudson R. and C. Phillips.

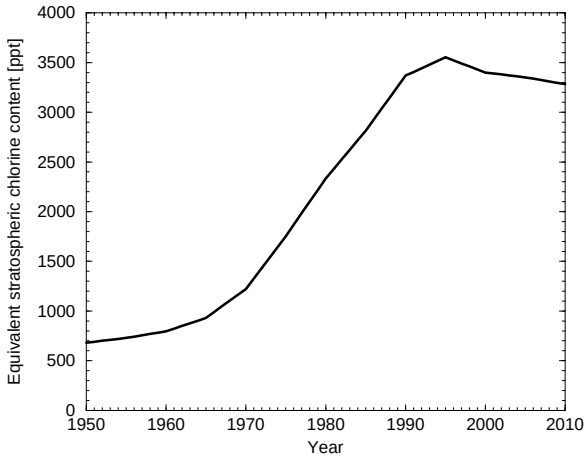

Figure 1: Equivalent chlorine content of the stratosphere in ppt for the heterogeneous chemistry part of the ozone source/sink parameterization (provided by Pascal Simon, Météo-France).

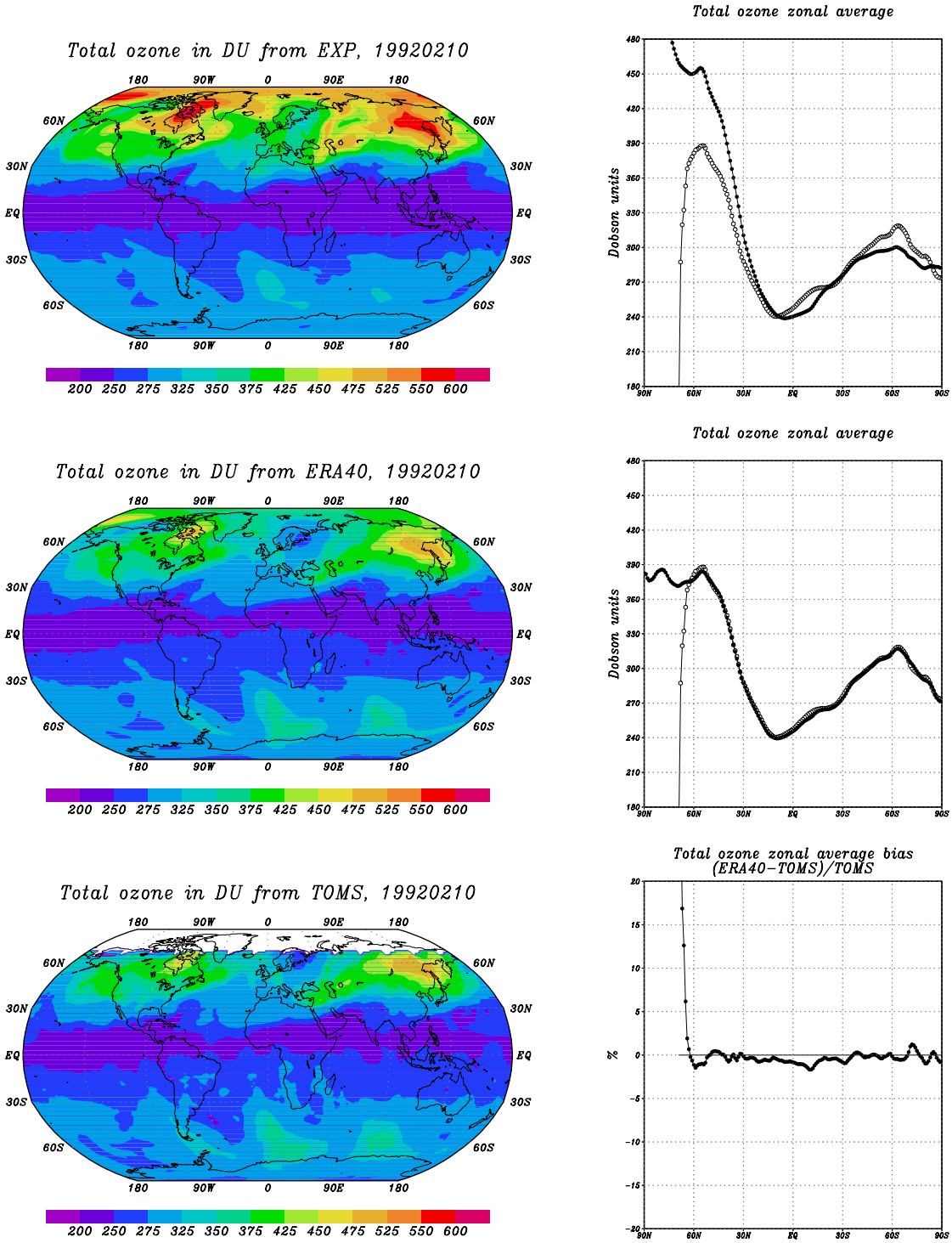

Figure 2: Colour plots: Total column ozone in DU on 10 February 1992 from a model run in which no ozone observations are assimilated (top), from the ERA-40 production in which TOMS total column ozone and SBUV ozone layers are assimilated (middle), and from gridded daily TOMS data (bottom). The top and the middle plot on the right show the zonal average total ozone values from the model (dark curve) and from the TOMS data (open circles). The bottom plot on the right shows the relative zonal mean difference between ERA-40 and the observations in %.

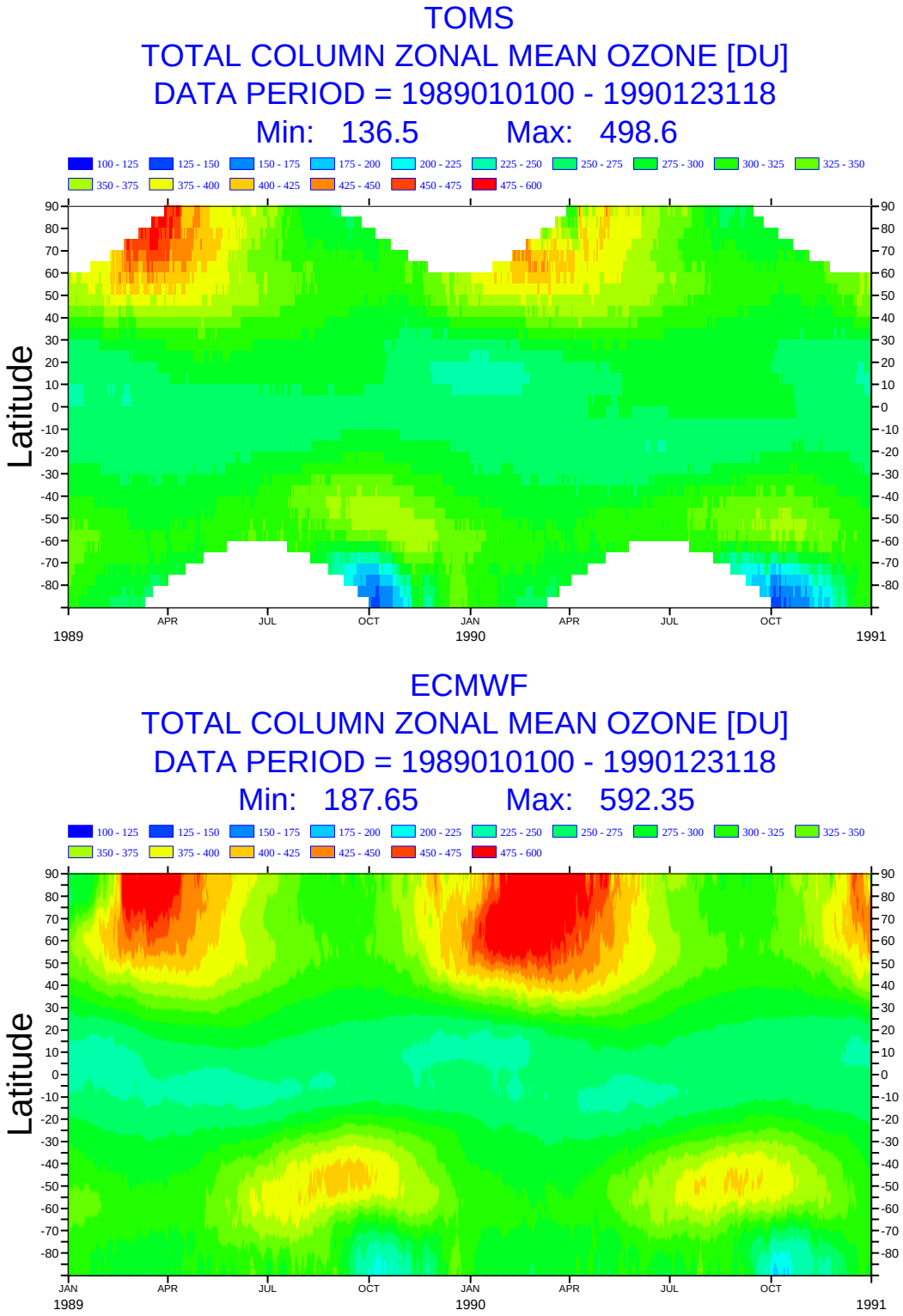

Figure 3: Time series of zonally averaged total column ozone in DU from 1989 to the end of 1990 from TOMS data (top) and ERA-40 (bottom).

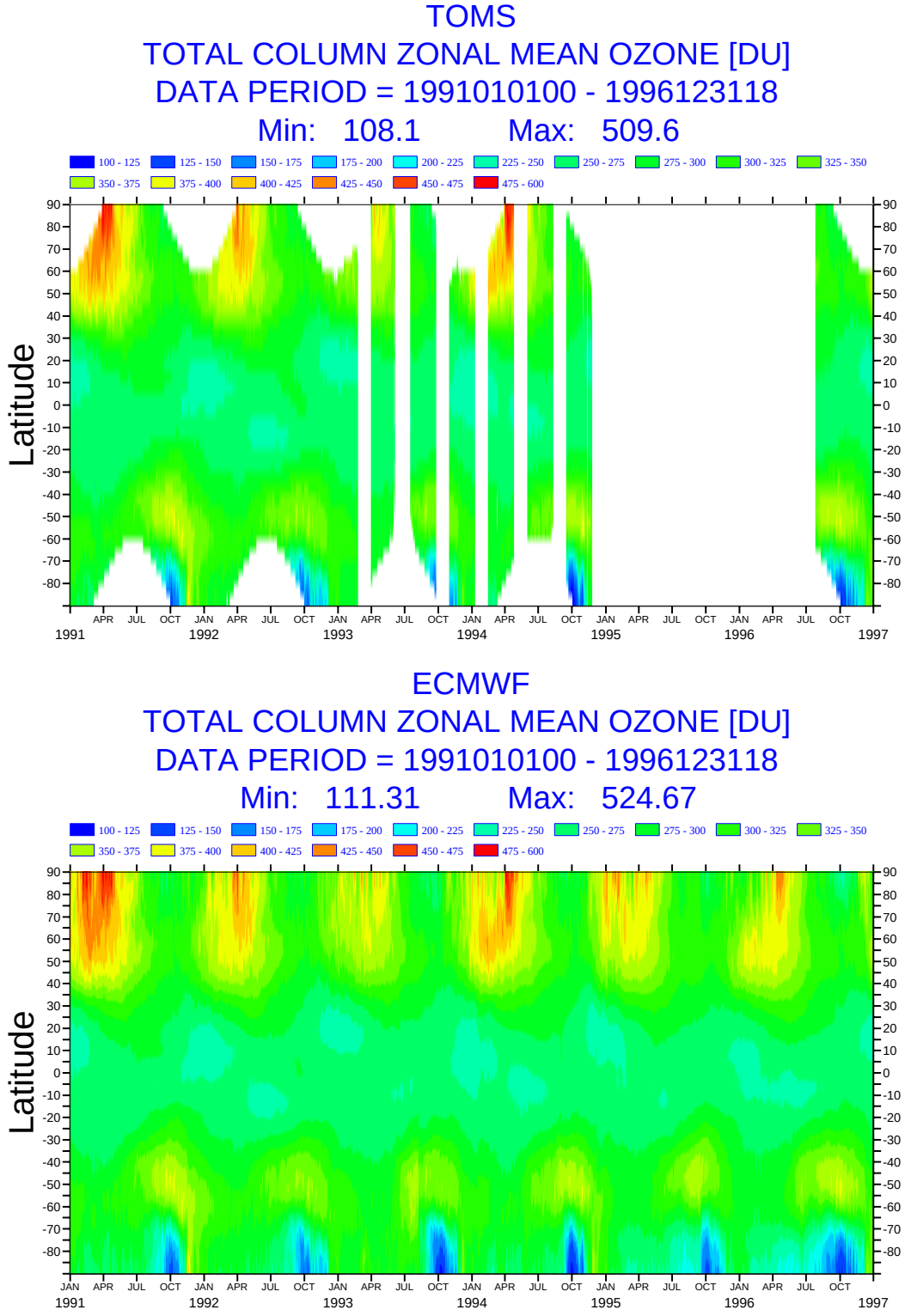

Figure 4: Time series of zonally averaged total column ozone in DU from 1991 to the end of 1996 from TOMS data (top) and ERA-40 (bottom).

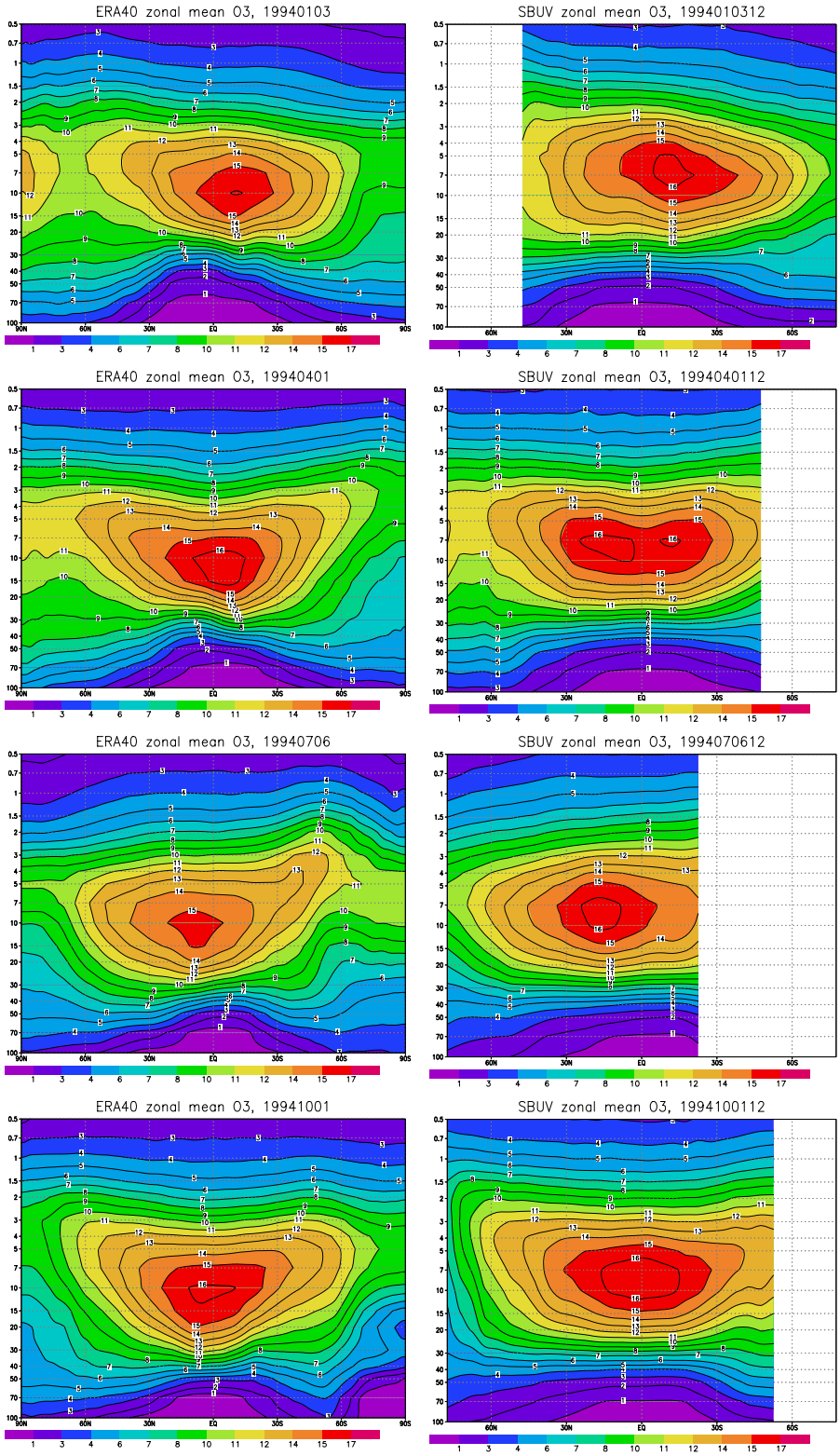

Figure 5: Vertical cross section of zonal mean ozone in ppmm on 3 January, 1 April, 6 July and 1 October 1994 from ERA-40 (left) and SBUV (right).

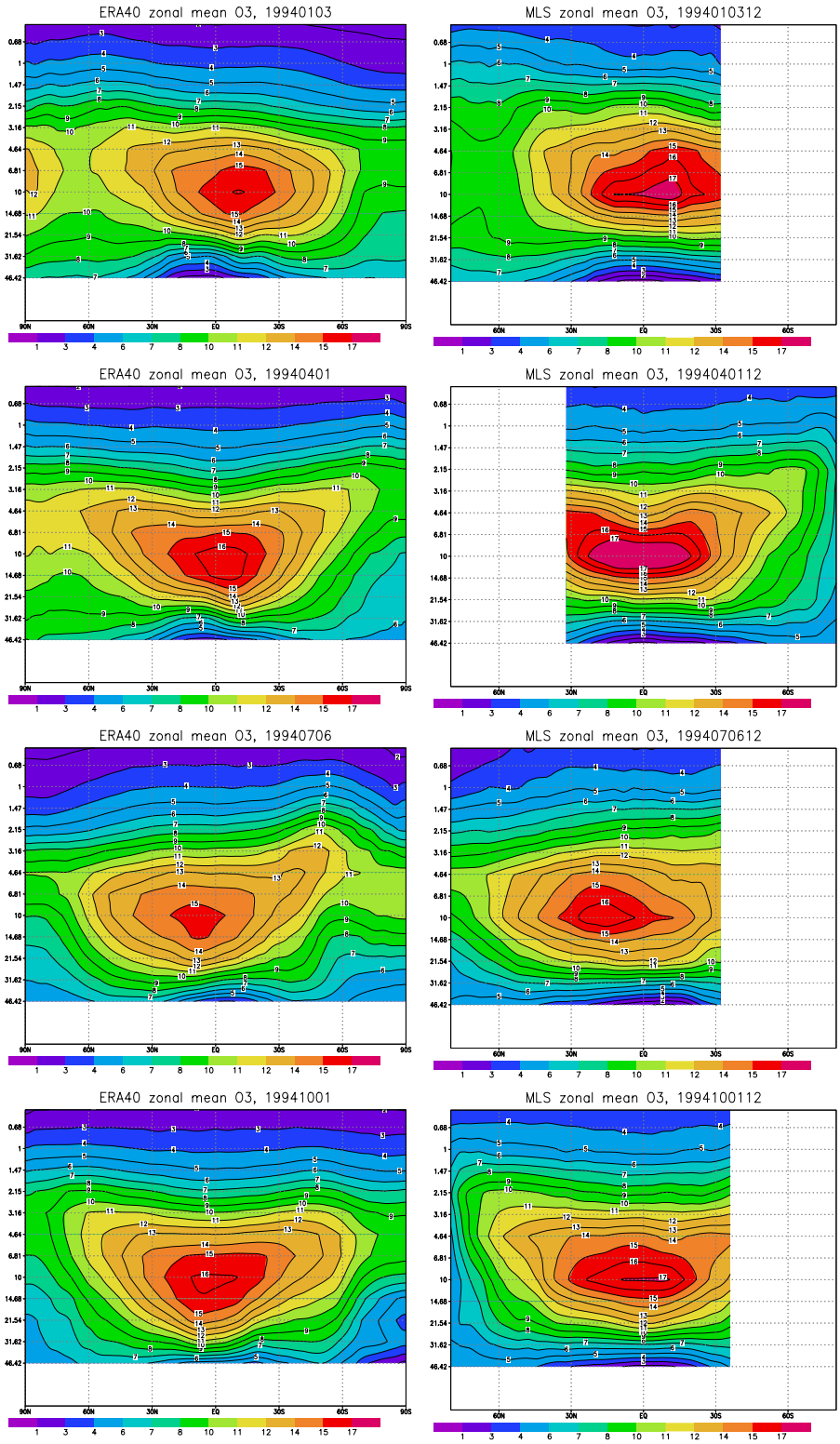

Figure 6: Vertical cross section of zonal mean ozone in ppmm on 3 January, 1 April, 6 July and 1 October 1994 from ERA-40 (left) and MLS data (right).

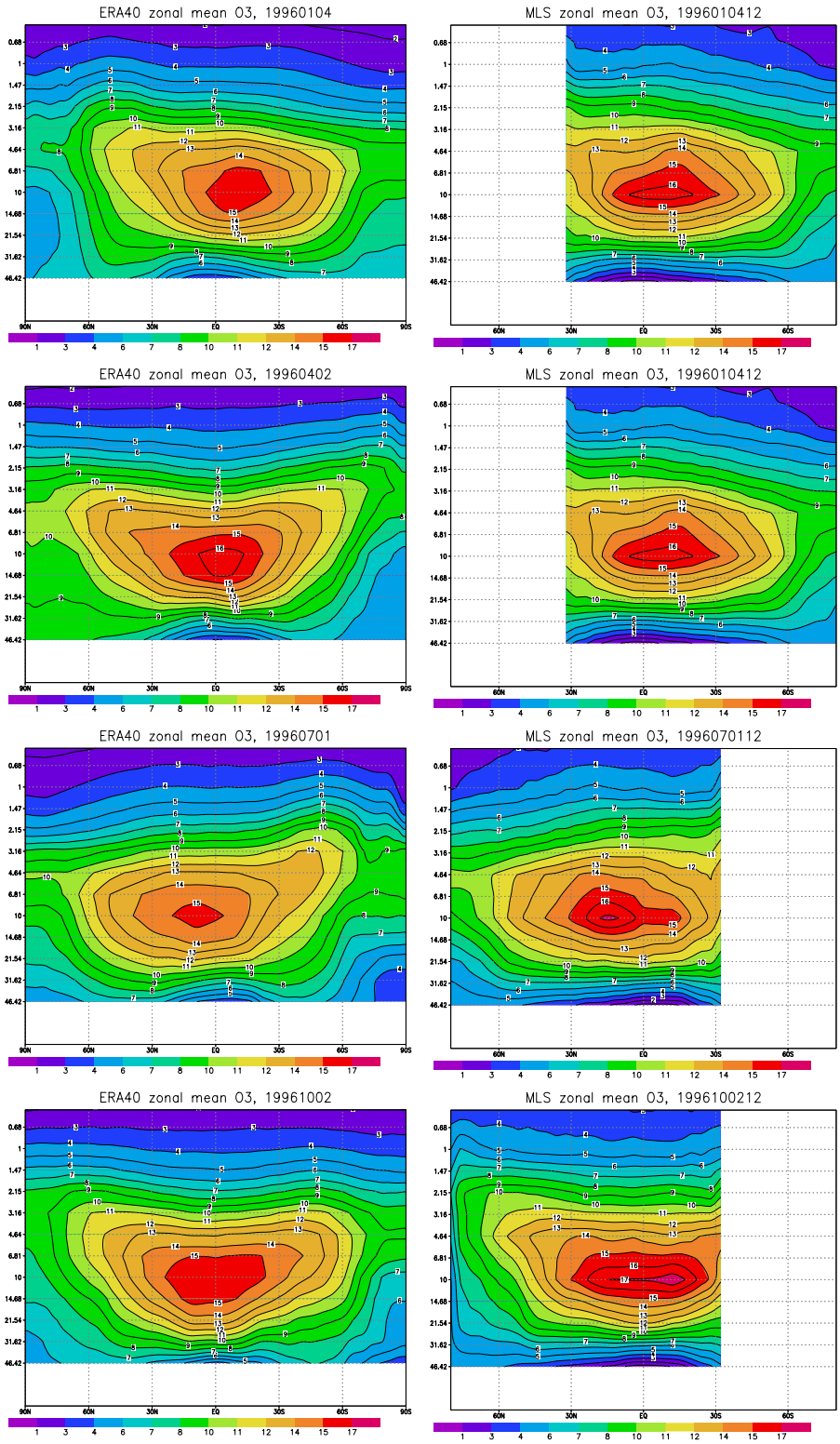

Figure 7: Vertical cross section of zonal mean ozone in ppmm on 4 January, 2 April, 1 July and 2 October 1996 from ERA-40 (left) and MLS data (right).

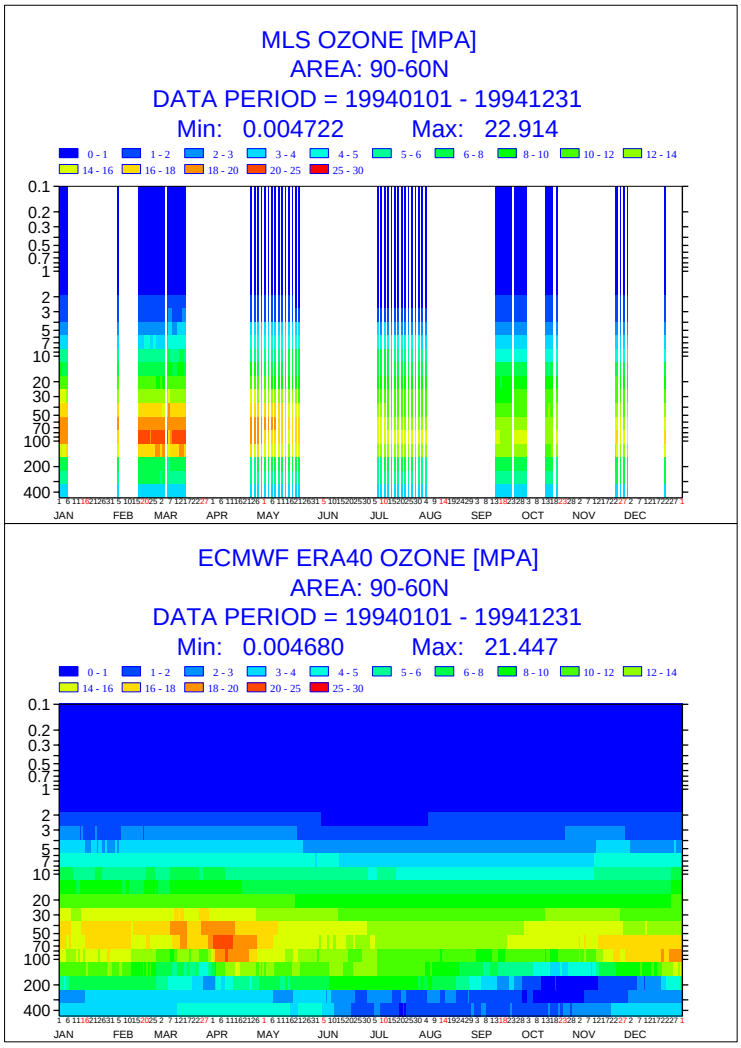

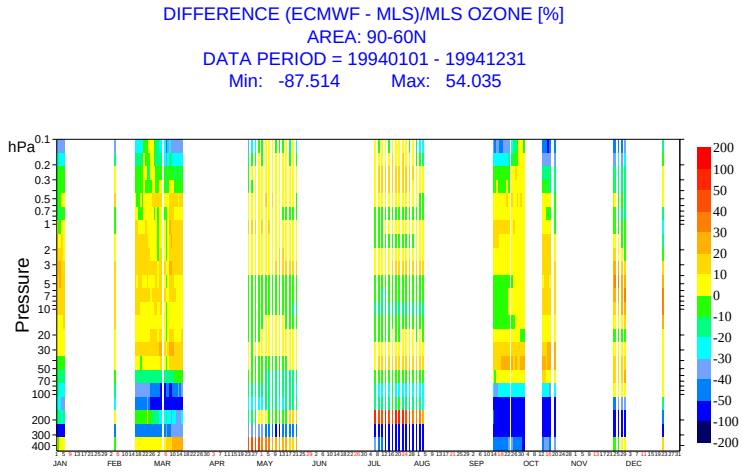

Figure 8: Timeseries of the stratospheric ozone averaged between 90-60° N from MLS data (top) and ERA (middle) in mPa for 1994. The bottom plot shows the relative difference in %.

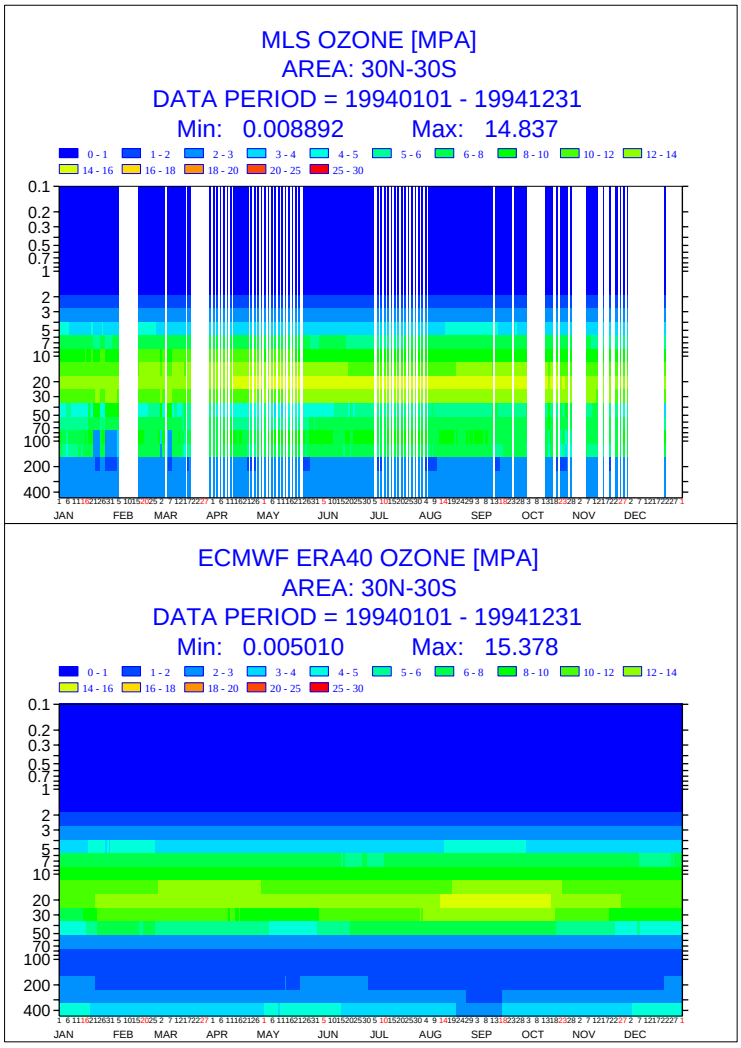

Figure 9: Timeseries of the stratospheric ozone averaged between 30° N-30° S from MLS data (top) and ERA (middle) in mPa for 1994. The bottom plot shows the relative difference in %.

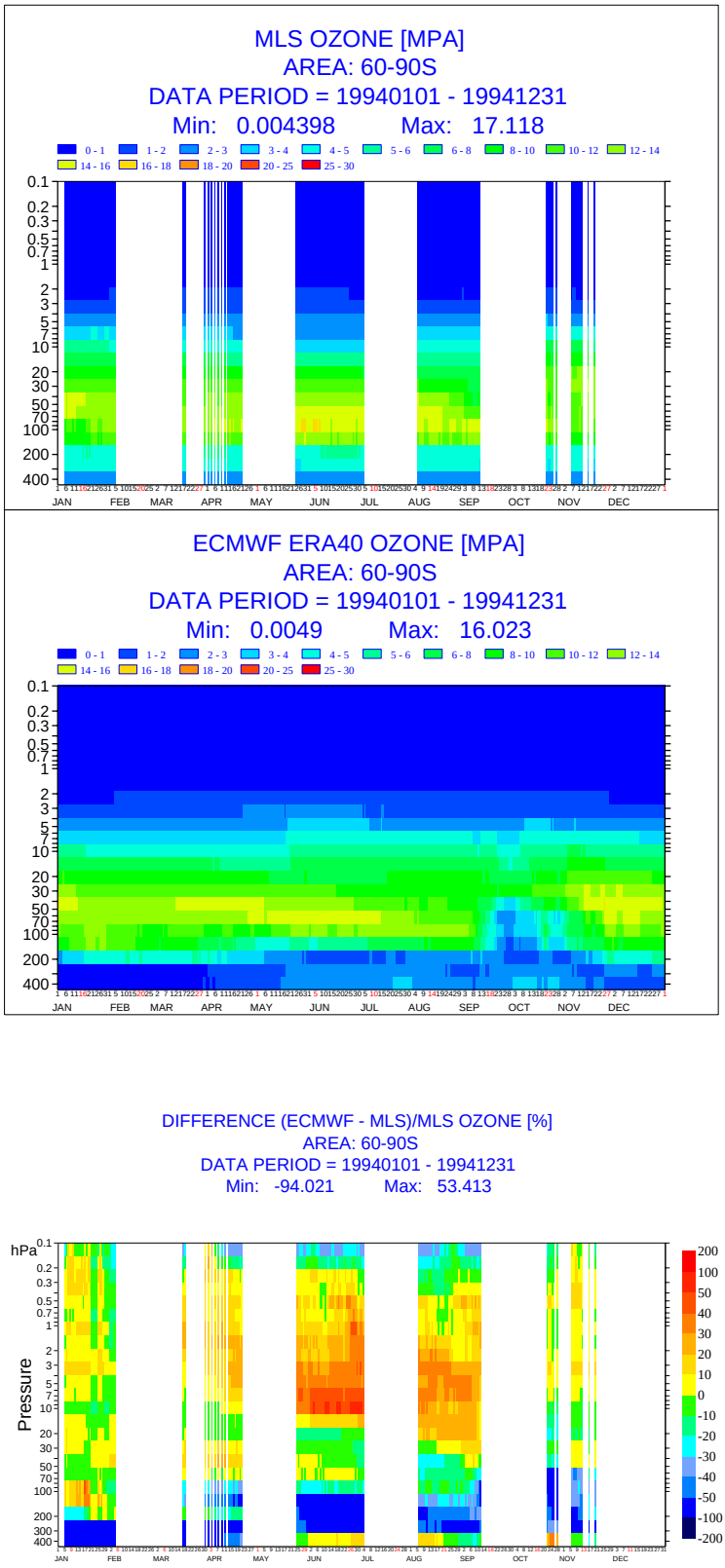

Figure 10: Timeseries of the stratospheric ozone averaged between 60-90°S from MLS data (top) and ERA (middle) in mPa for 1994. The bottom plot shows the relative difference in %.

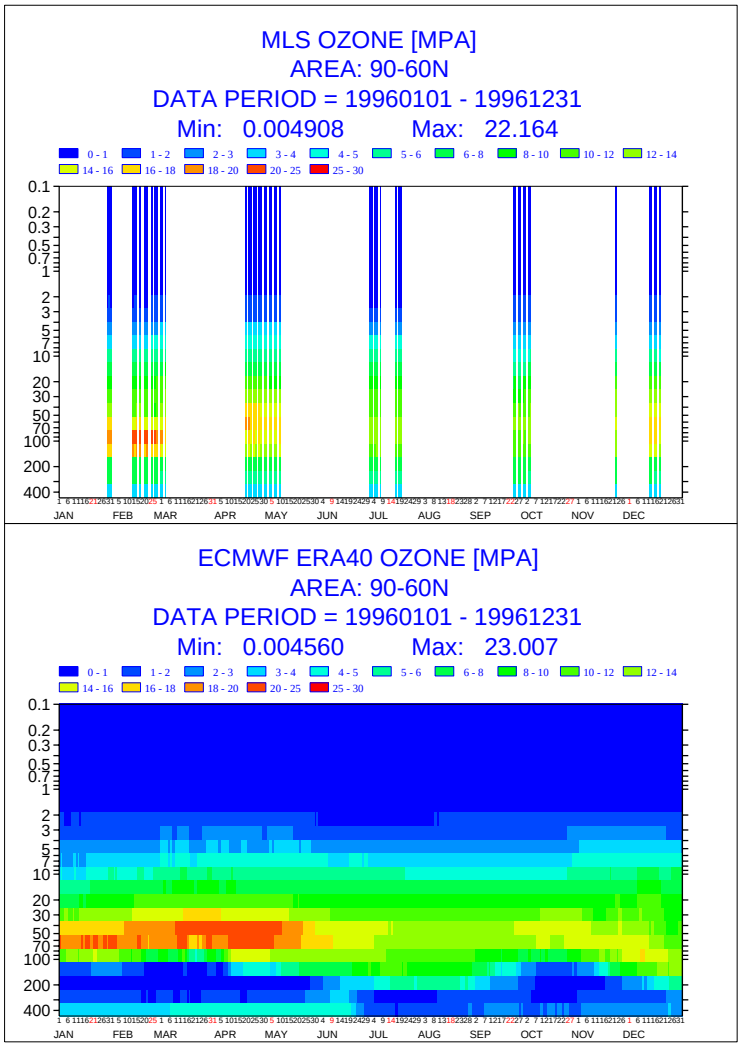

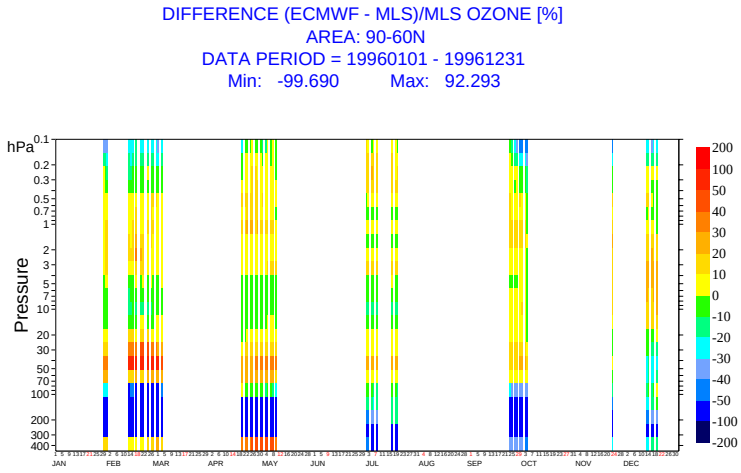

Figure 11: Timeseries of the stratospheric ozone averaged between 90-60° N from MLS data (top) and ERA (middle) in mPa for 1996. The bottom plot shows the relative difference in %.

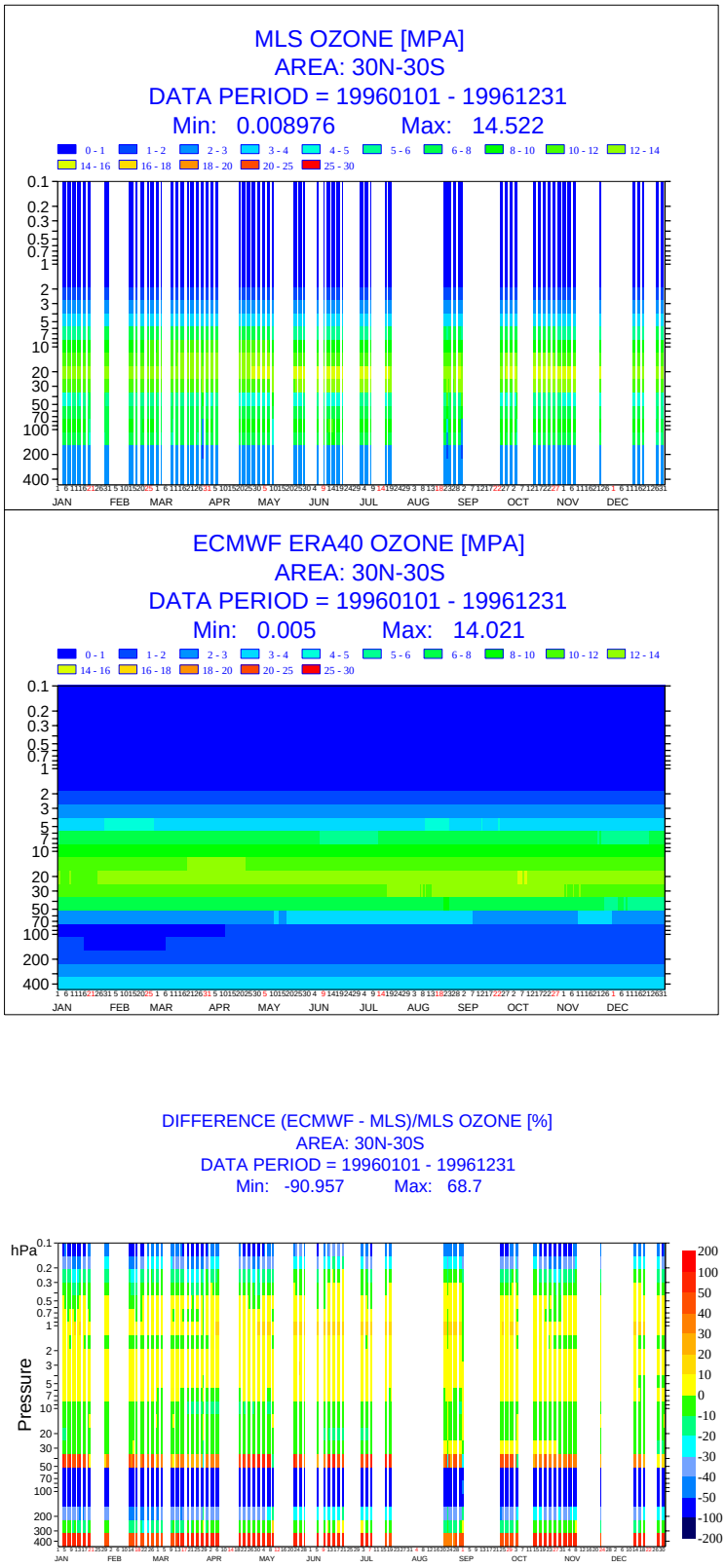

Figure 12: Timeseries of the stratospheric ozone averaged between 30°N-30°S from MLS data (top) and ERA (middle) in mPa for 1996. The bottom plot shows the relative difference in %.

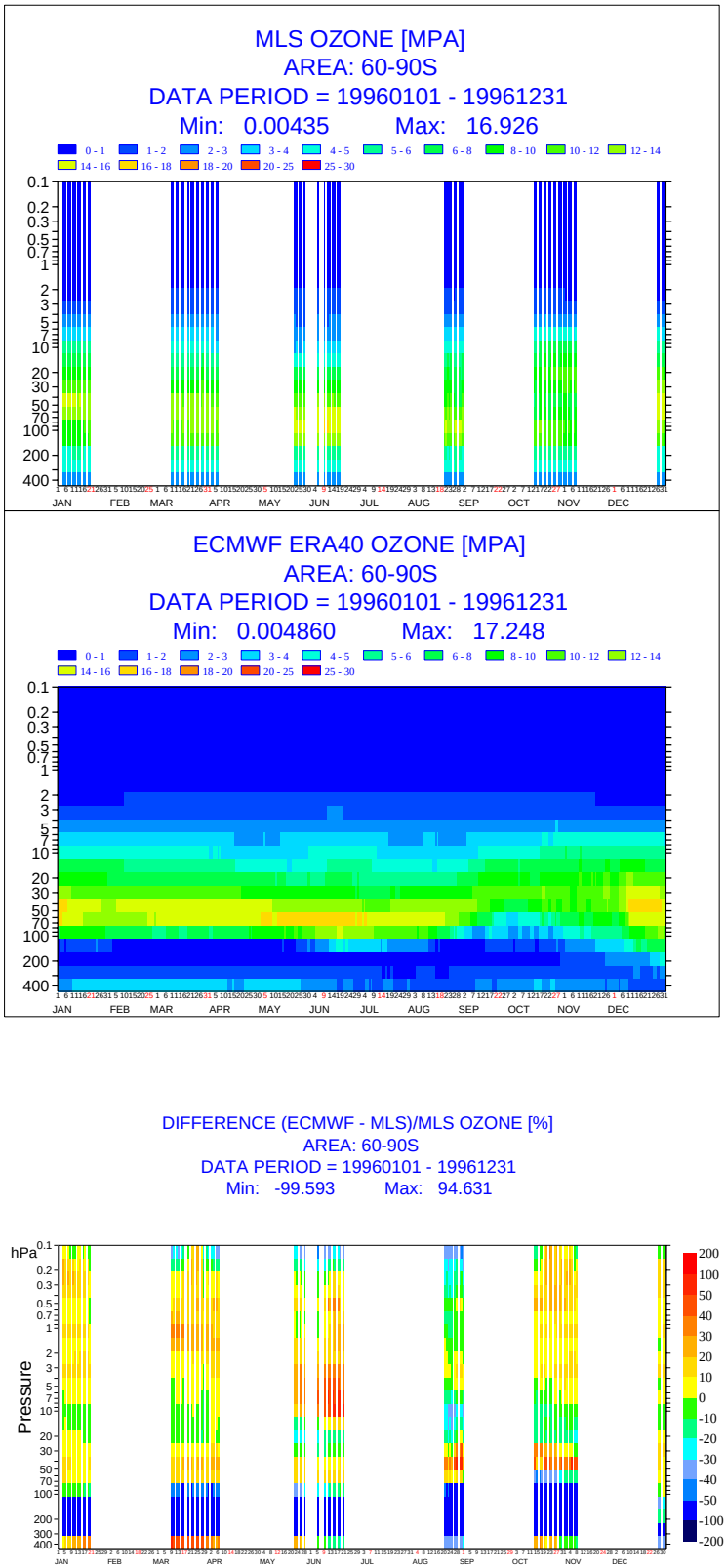

Figure 13: Timeseries of the stratospheric ozone averaged between 60-90°S from MLS data (top) and ERA (middle) in mPa for 1996. The bottom plot shows the relative difference in %.

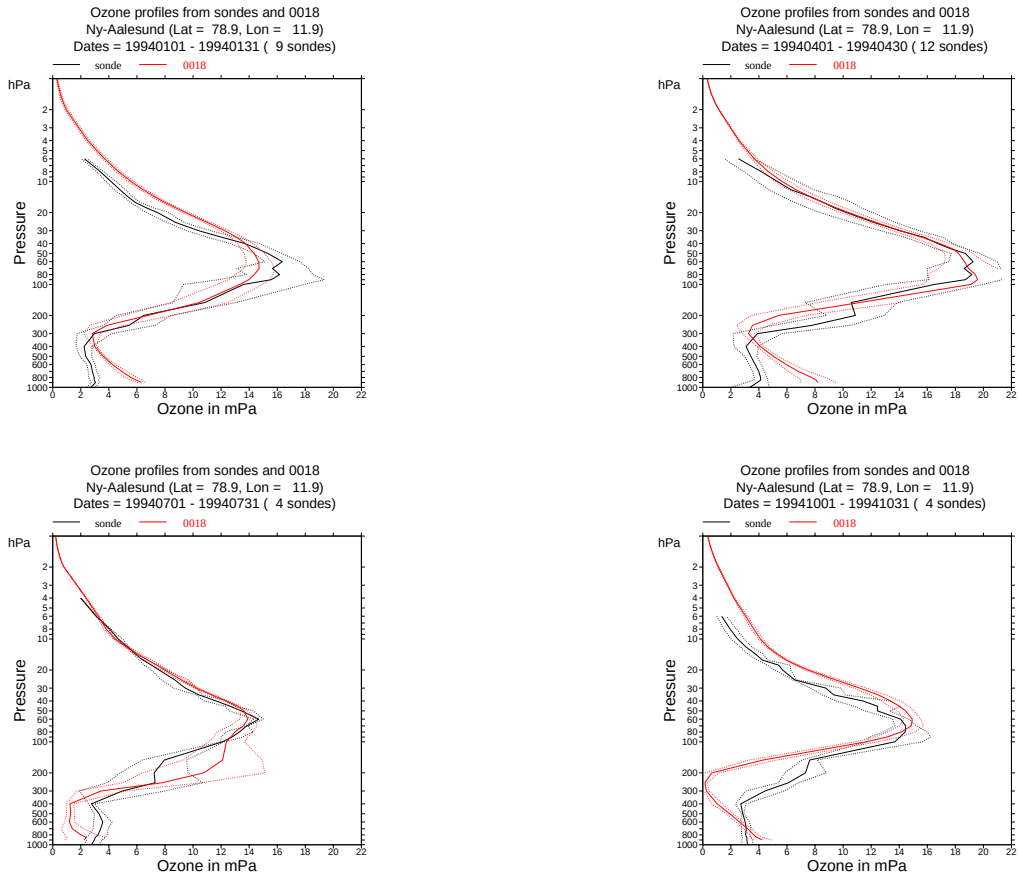

Figure 14: Ozone profiles in mPa at Ny-Aalesund from sondes (black curves) and ERA-40 (red curves) for January, April, July and October 1994. The solid line is the mean profile, the dotted lines +/- one standard deviation.

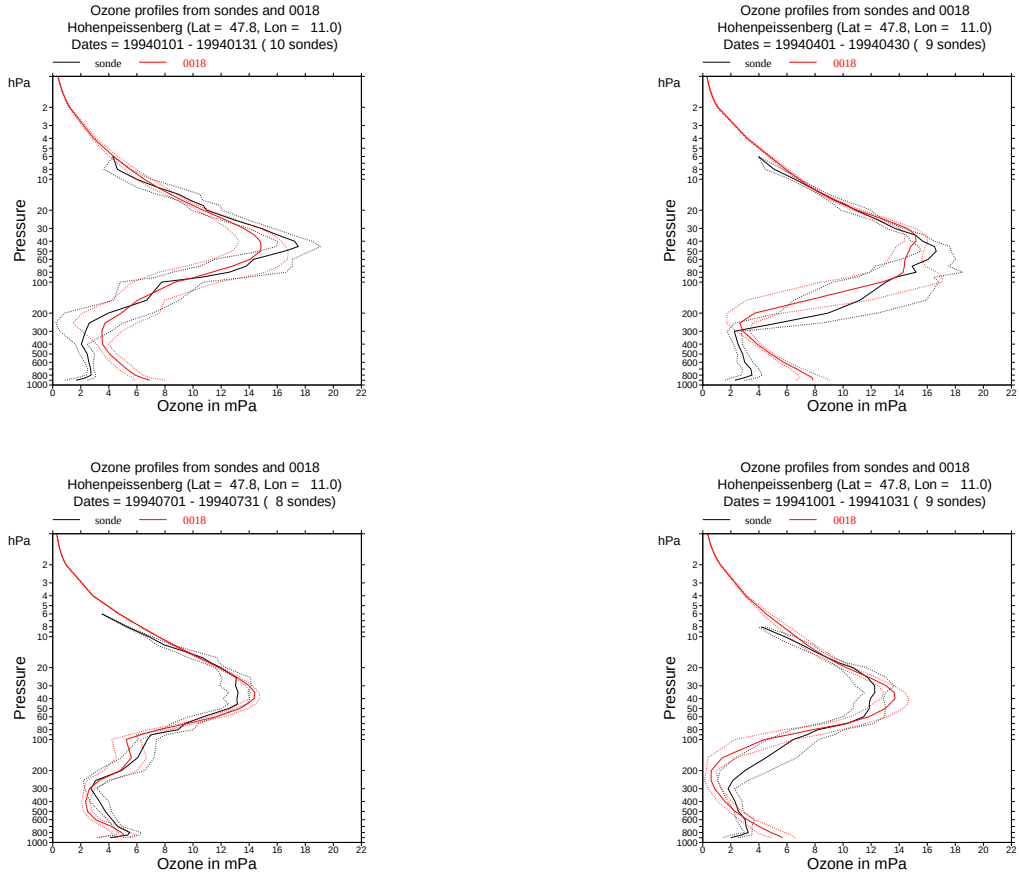

Figure 15: Ozone profiles in mPa at Hohenpeissenberg from sondes (black curves) and ERA-40 (red curves) for January, April, July and October 1994. The solid line is the mean profile, the dotted lines +/- one standard deviation.

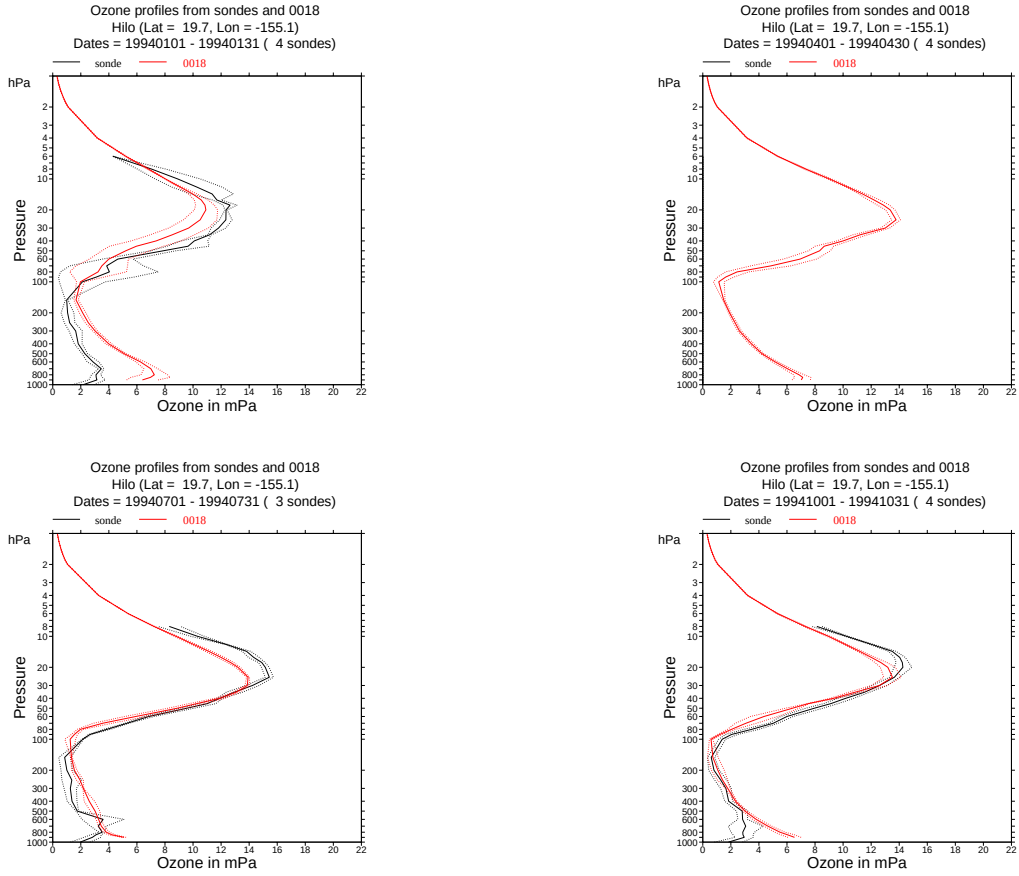

Figure 16: Ozone profiles in mPa at Hilo from sondes (black curves) and ERA-40 (red curves) for January, April, July and October 1994. The solid line is the mean profile, the dotted lines +/- one standard deviation.

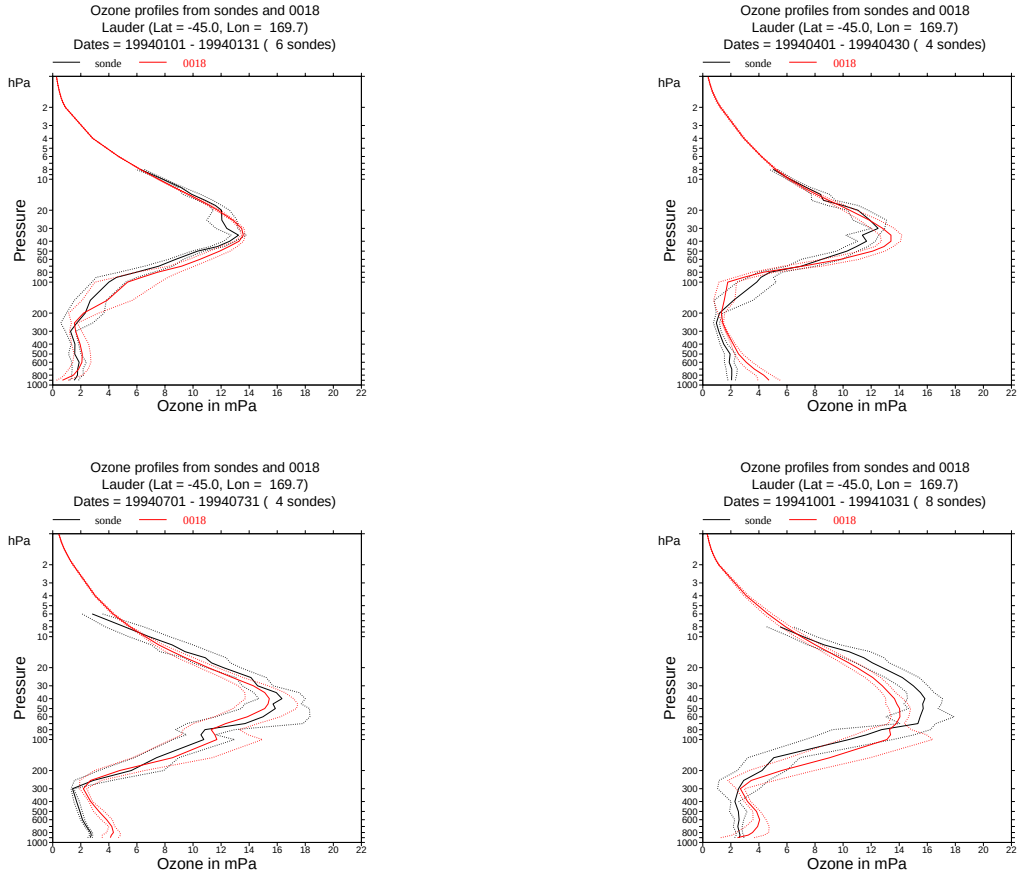

Figure 17: Ozone profiles in mPa at Lauder from sondes (black curves) and ERA-40 (red curves) for January, April, July and October 1994. The solid line is the mean profile, the dotted lines +/- one standard deviation.

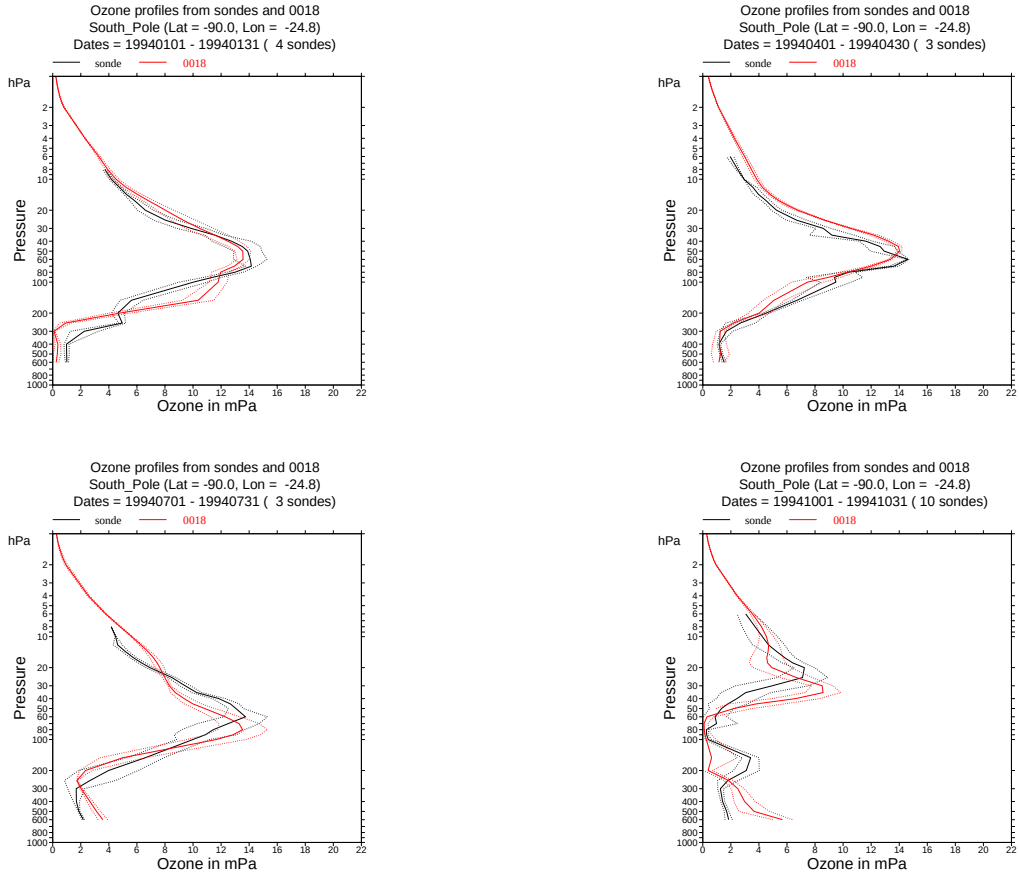

Figure 18: Ozone profiles in mPa at the South Pole from sondes (black curves) and ERA-40 (red curves) for January, April, July and October 1994. The solid line is the mean profile, the dotted lines +/- one standard deviation.

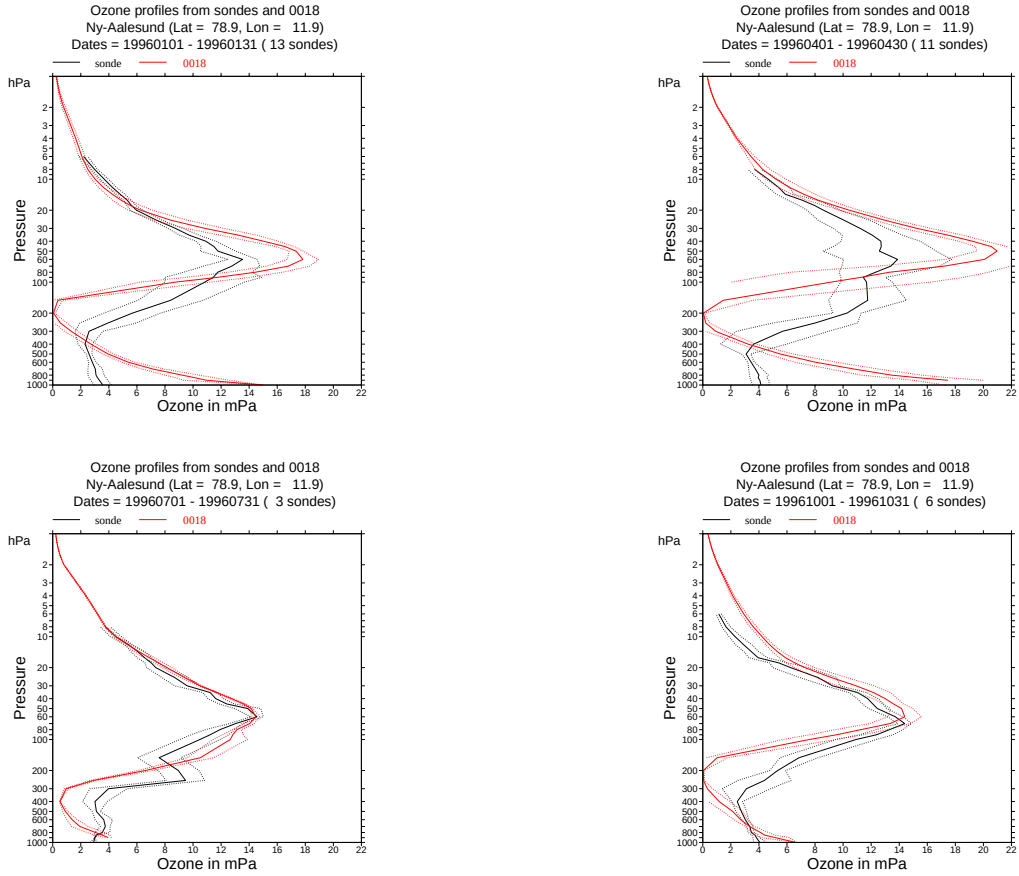

Figure 19: Ozone profiles in mPa at Ny-Aalesund from sondes (black curves) and ERA-40 (red curves) for January, April, July and October 1996. The solid line is the mean profile, the dotted lines +/- one standard deviation.

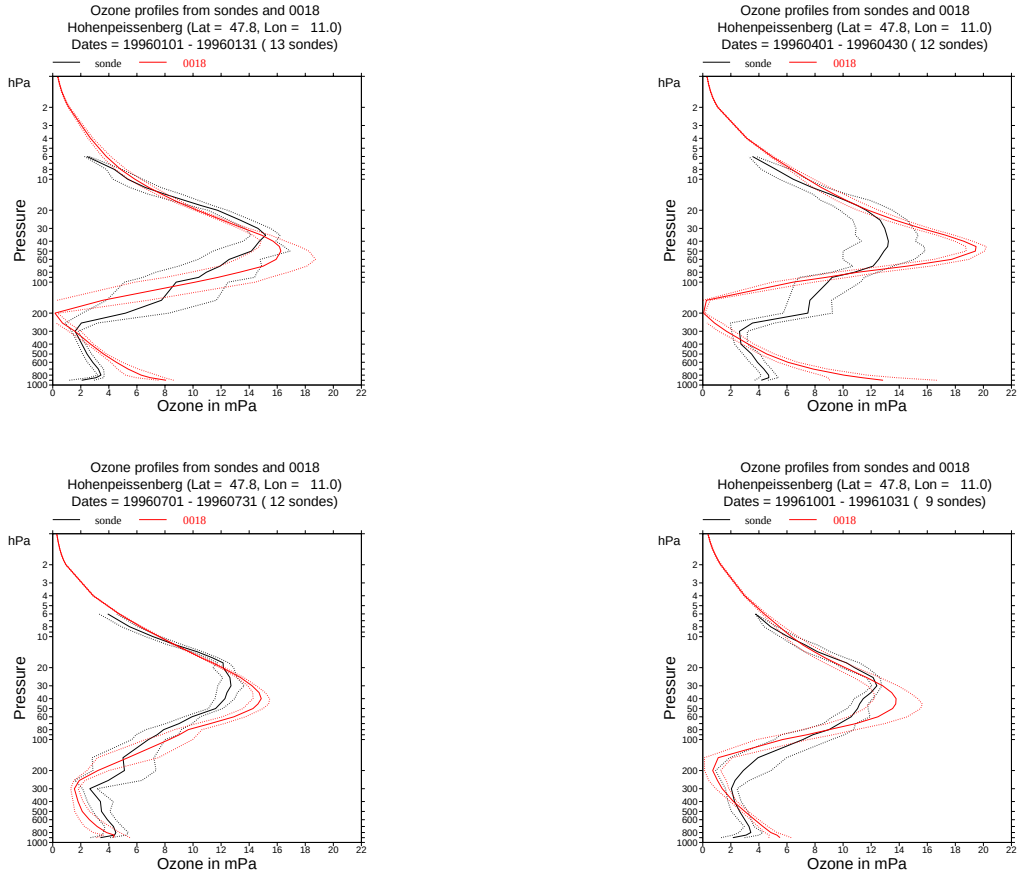

Figure 20: Ozone profiles in mPa at Hohenpeissenberg from sondes (black curves) and ERA-40 (red curves) for January, April, July and October 1996. The solid line is the mean profile, the dotted lines +/- one standard deviation.

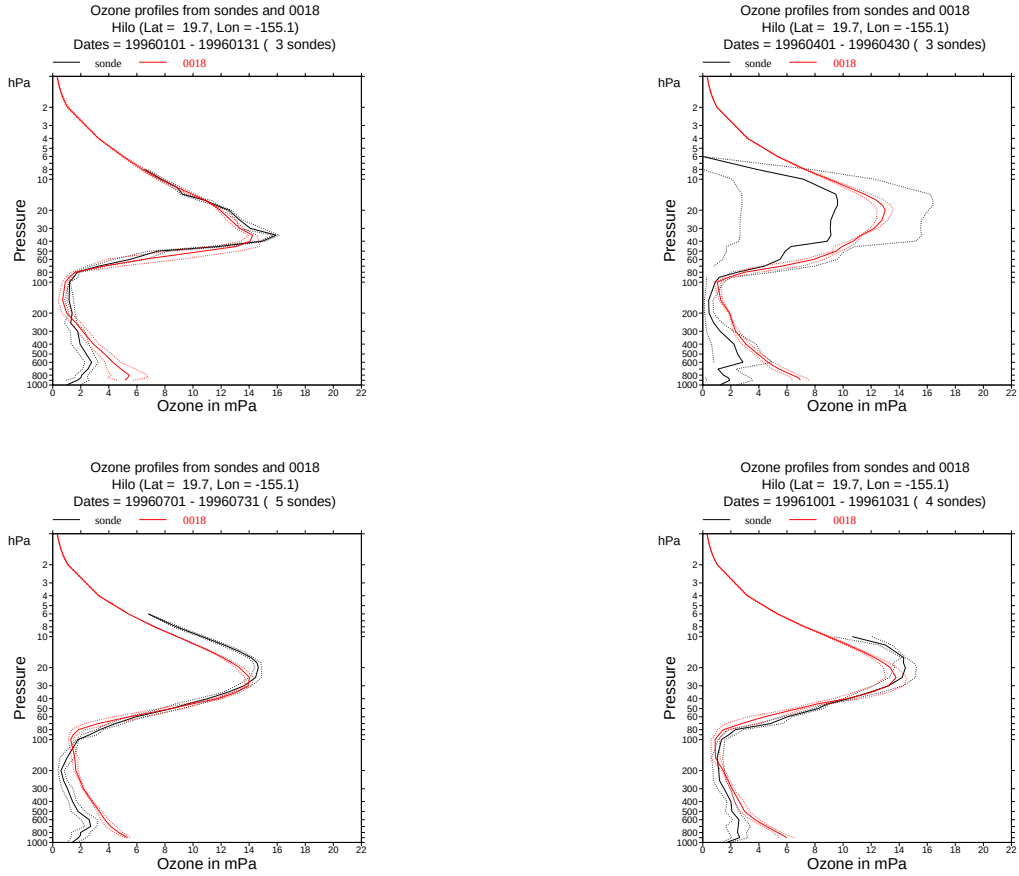

Figure 21: Ozone profiles in mPa at Hilo from sondes (black curves) and ERA-40 (red curves) for January, April, July and October 1996. The solid line is the mean profile, the dotted lines +/- one standard deviation.

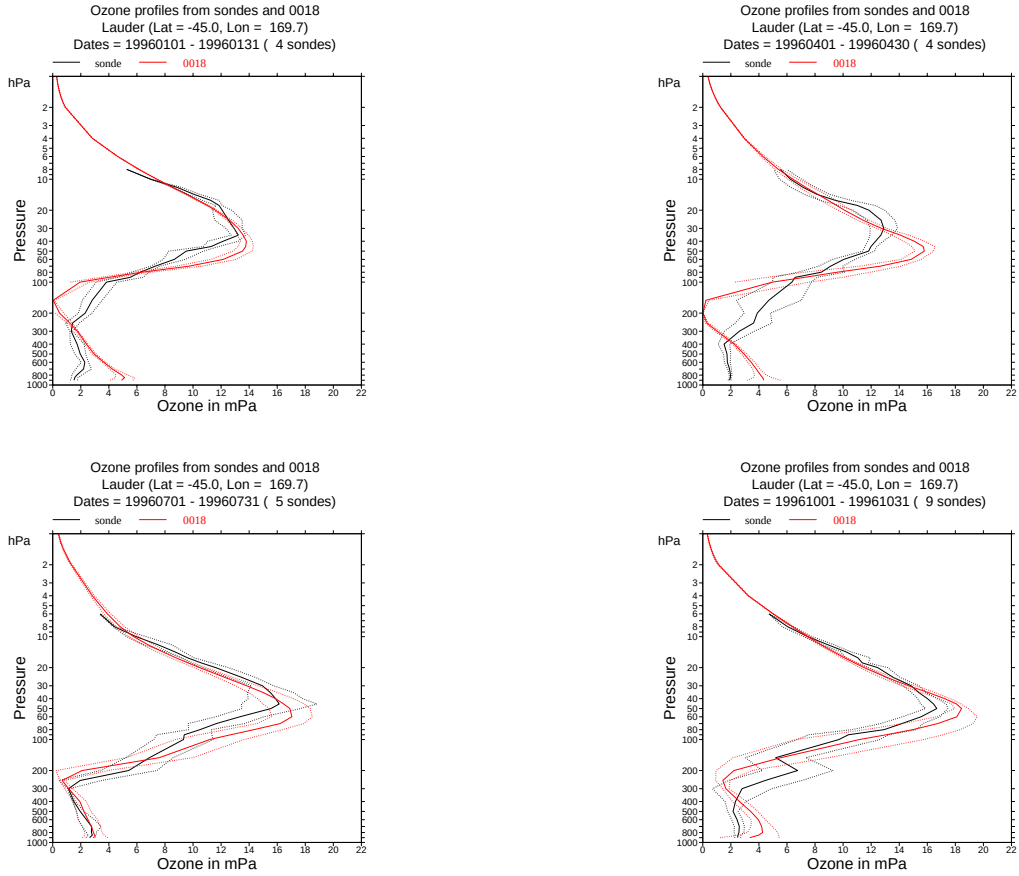

Figure 22: Ozone profiles in mPa at Lauder from sondes (black curves) and ERA-40 (red curves) for January, April, July and October 1996. The solid line is the mean profile, the dotted lines +/- one standard deviation.

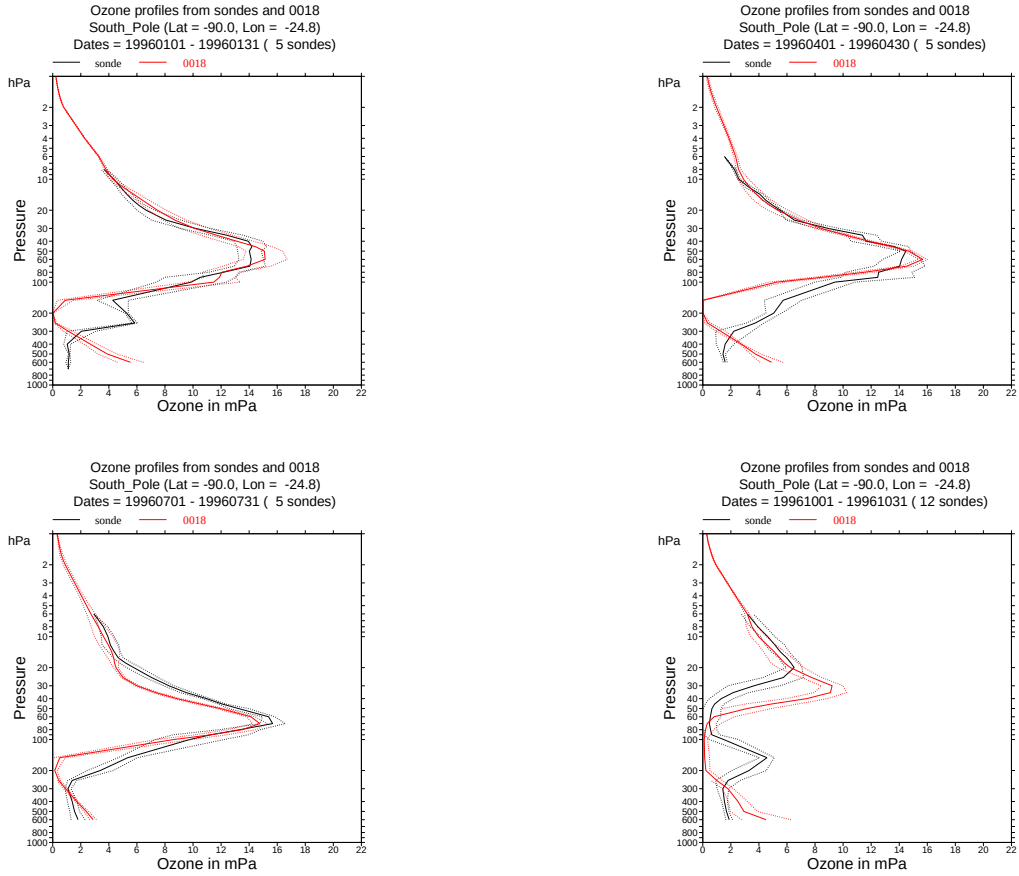

Figure 23: Ozone profiles in mPa at the South Pole from sondes (black curves) and ERA-40 (red curves) for January, April, July and October 1996. The solid line is the mean profile, the dotted lines +/- one standard deviation.

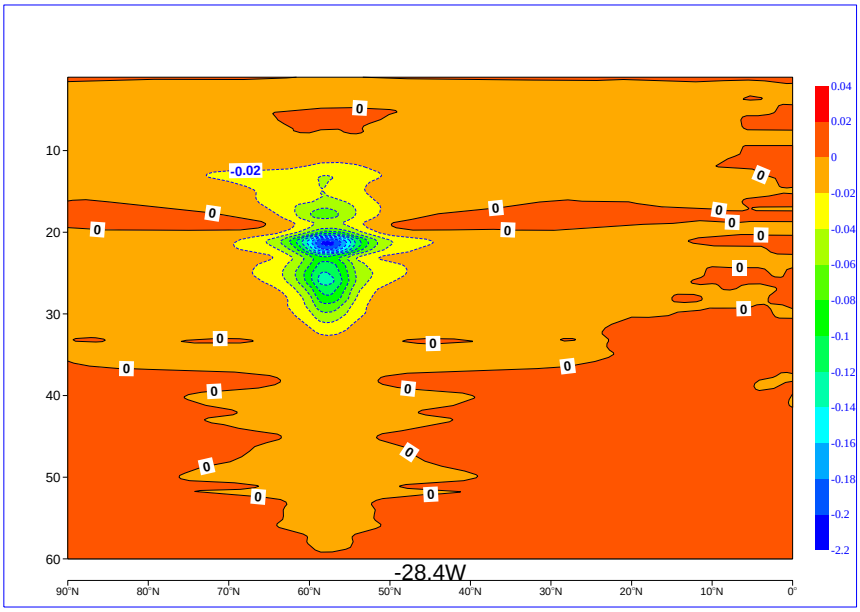

Figure 24: Vertical cross section at 28.4°E of the analysis increment (in ppmm) created by a single TOMS observation placed at 57.56 latitude, -28.38 longitude on 25 January 1992 at 11:19 in Exp-A. The observation has a value of 247 DU and is 66.7 DU lower than the background. The vertical axis is model levels.

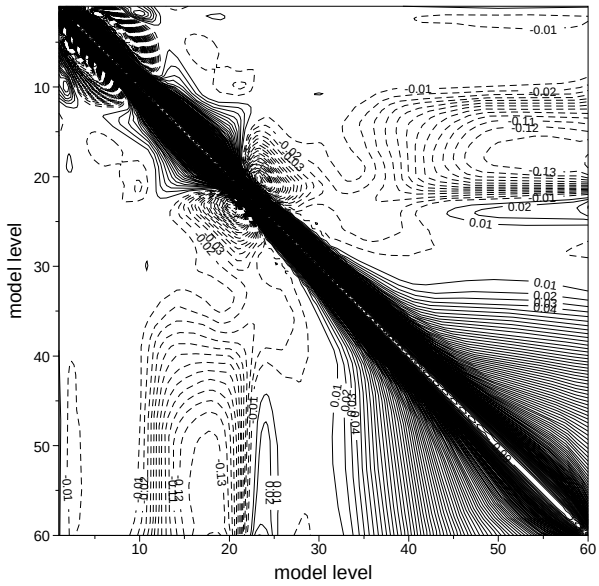

Figure 25: Wavenumber averaged vertical correlation matrix for ozone, which is used in ERA-40 until October 1996.

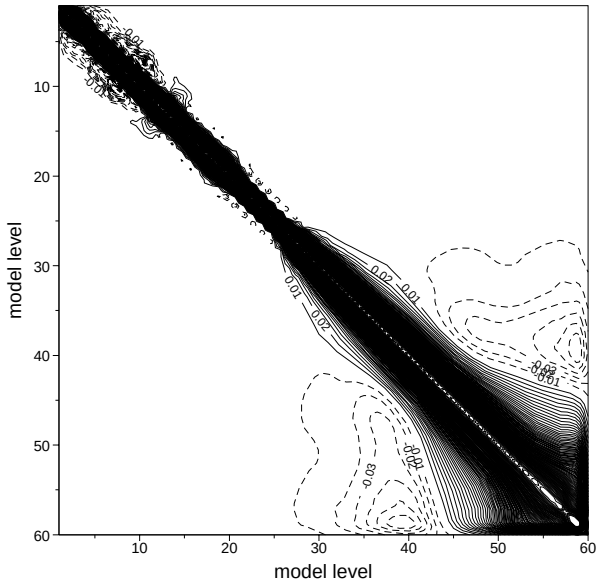

Figure 26: Wavenumber averaged vertical correlation matrix for ozone, which is used in ERA-40 after October 1996.

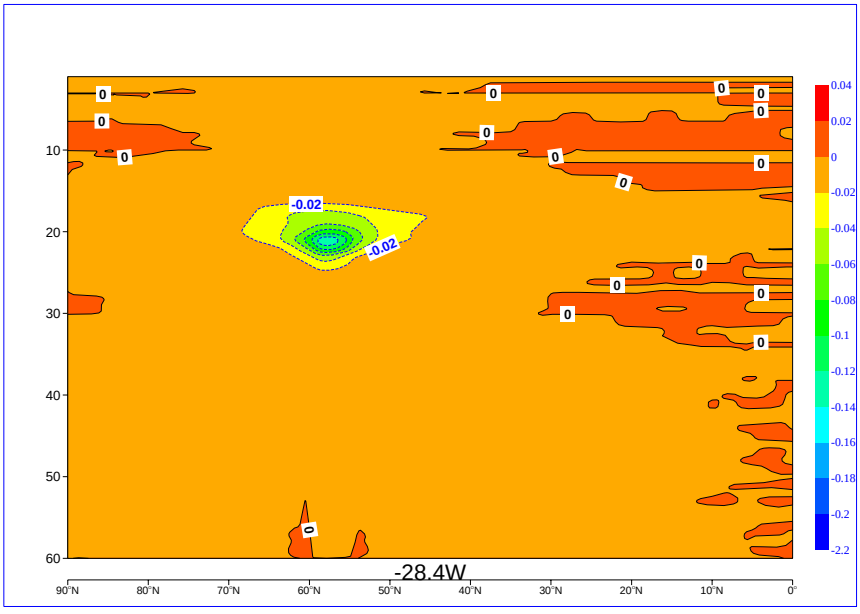

Figure 27: Vertical cross section at 28.4°E of the analysis increment (in ppmm) created by a single TOMS observation placed at 57.56 latitude, -28.38 longitude on 25 January 1992 at 11:19 in Exp-B. The observation has a value of 247 DU and is 66.7 DU lower than the background. The vertical axis is model levels.

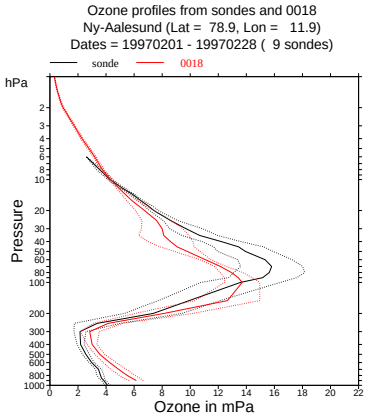

Figure 28: Ozone profile in mPa at Ny-Aalesund from sondes (black curves) and ERA-40 (red curves) for February 1997. The solid line is the mean profile, the dotted lines +/- one standard deviation.